Arterial smooth muscle cell PKD2 (TRPP1) channels regulate systemic blood pressure

Simon Bulley[#], Carlos Fernández-Peña[#], Raquibul Hasan, M. Dennis Leo, Padmapriya Muralidharan, Charles E. MacKay, Kirk W. Evanson, Luiz Moreira-Junior, Alejandro Mata-Daboin, Sarah K. Burris, Qian Wang, Korah P. Kuruvilla and Jonathan H. Jaggar*

from the

Department of Physiology,
University of Tennessee Health Science Center,
Memphis, TN 38163, USA

Short title: Arterial myocyte PKD2 controls blood pressure

* To whom correspondence should be addressed:
Jonathan H. Jaggar, PhD
Department of Physiology
University of Tennessee Health Science Center
847 Monroe Ave
Memphis, TN 38163

E-mail: jjaggar@uthsc.edu
Tel: (901) 448-1208
Fax: (901) 448-7126
email: jjaggar@uthsc.edu

Authorship Note: [#] S.B and C.F-P. contributed equally to this work

Short Title: PKD2 channels regulate blood pressure

Abstract

Systemic blood pressure is determined, in part, by arterial smooth muscle cells (myocytes). Several Transient Receptor Potential (TRP) channels are proposed to be expressed in arterial myocytes, but it is unclear if these proteins control physiological blood pressure and contribute to hypertension *in vivo*. We generated the first inducible, smooth muscle-specific knockout mice for a TRP channel, namely for PKD2 (TRPP1), to investigate arterial myocyte and blood pressure regulation by this protein. Using this model, we show that intravascular pressure and α_1-adrenoceptors activate PKD2 channels in arterial myocytes of different systemic organs. PKD2 channel activation in arterial myocytes leads to an inward Na^+ current, membrane depolarization and vasoconstriction. Inducible, smooth muscle cell-specific PKD2 knockout lowers both physiological blood pressure and hypertension and prevents pathological arterial remodeling during hypertension. Thus, arterial myocyte PKD2 controls systemic blood pressure and targeting this TRP channel reduces high blood pressure.

Introduction

Systemic blood pressure is controlled by total peripheral resistance, which is determined by the diameter of small arteries and arterioles. Arterial smooth muscle cell (myocyte) contraction reduces luminal diameter, leading to an increase in systemic blood pressure, whereas relaxation results in vasodilation that decreases blood pressure. Membrane potential is a primary determinant of arterial contractility [1]. Depolarization activates myocyte voltage-dependent calcium (Ca^{2+}) channels (Ca_V), leading to an increase in intracellular Ca^{2+} concentration $[Ca^{2+}]_i$ and vasoconstriction. In contrast, hyperpolarization reduces $[Ca^{2+}]_i$, resulting in vasodilation [1]. *In vitro* studies have identified several different types of ion channel that regulate the membrane potential and contractility of arterial myocytes, but whether many of these ion channels regulate systemic blood pressure is unclear. Given that hypertension is associated with altered arterial contractility, myocyte ion channels that contribute to high blood pressure are also important to determine.

Transient Receptor Potential (TRP) channels constitute a family of ~28 proteins that are subdivided into 6 different classes, including polycystin (TRPP), canonical (TRPC), vanilloid (TRPV), ankyrin (TRPA), and melastatin (TRPM) [2]. Experiments performed using cultured and non-cultured cells and whole arteries, which contain multiple different cell types, have suggested that approximately thirteen different TRP channels may be expressed in arterial myocytes, including PKD2 (also termed TRPP1), TRPC1, TRPC3-6, TRPV1-4, TRPA1, TRPM4 and TRPM8 [2]. In many of these studies, TRP channel expression was reported in myocytes of vasculature that does not control systemic blood pressure, including conduit vessels, cerebral arteries, portal vein and pulmonary arteries [2]. Blood pressure measurements in constitutive, global TRPC6, TRPM4 and TRPV4 channel knockout mice produced inconsistent results or generated complex findings that were associated with compensatory mechanisms [3-6]. Thus, the contribution of arterial myocyte TRP channels to physiological systemic blood pressure and pathological changes in blood pressure are unclear. Also uncertain is whether TRP channel subtypes present in arterial myocytes of different organs are similarly regulated by physiological stimuli and if such modulation leads to the same functional outcome.

PKD2 is a six transmembrane domain protein with cytoplasmic N and C termini [7]. PKD2 is expressed in myocytes of rat and human cerebral arteries, mouse and human mesenteric arteries and in porcine whole aorta [8-10]. RNAi-mediated knockdown of PKD2 inhibited pressure-induced vasoconstriction (myogenic tone) in cerebral arteries [10 11]. In global, constitutive $PKD2^{+/-}$ mice, an increase in actin and myosin expression lead to larger phenylephrine-induced contractions in aorta and mesenteric arteries [12, 13]. It has also been proposed that arterial myocyte PKD2 channels inhibit

myogenic tone in mesenteric arteries [11]. Thus, *in vitro* studies have generated variable findings regarding physiological functions of arterial myocyte PKD2 channels.

Here, we generated an inducible, myocyte-specific PKD2 knockout mouse to investigate blood pressure regulation by this TRP channel. We show that inducible and cell-specific PKD2 channel knockout in myocytes reduces systemic blood pressure. We demonstrate that intravascular pressure and α_1-adrenoceptor activation activate myocyte PKD2 channels in systemic arteries of different tissues, leading to an inward sodium current (I_{Na}), membrane depolarization and vasoconstriction. We also show that PKD2 channels are upregulated during hypertension and that myocyte PKD2 knockout causes vasodilation, attenuates remodeling of the arterial wall and reduces high blood pressure during hypertension. In summary, our study indicates that PKD2 channels in systemic artery myocytes control physiological blood pressure and are upregulated during hypertension, contributing to the blood pressure elevation.

Results

Generation of tamoxifen-inducible smooth muscle-specific PKD2 knockout mice

Mice with *loxP* sites flanking exons 11 and 13 (*Pkd2*$^{fl/fl}$) of the *Pkd2* gene were crossed with tamoxifen-inducible *Myh11-cre/ERT2* mice, producing a *Pkd2*$^{fl/fl}$*:Myh11-cre/ERT2* line. Genotyping was performed using a 3-primer (a, b, c) strategy to identify wild-type (in C57BL/6J), floxed and deleted PKD2 alleles. PCR of genomic DNA from mesenteric and hindlimb arteries of wild-type mice that lack *loxP* sites produced a 232 bp transcript (Figure 1 - figure supplement 1). Tamoxifen-treated *Pkd2*$^{fl/fl}$ mouse arteries and aorta produced a transcript of 318 bp, which arose from primers a and b (Figure 1 - supplement 1). PCR amplified a 209 bp transcript in vasculature from tamoxifen-treated *Pkd2*$^{fl/fl}$*:Myh11-cre/ERT2* mice due to primers a and c, confirming loss of the primer b annealing site. PCR of vasculature in *Pkd2*$^{fl/fl}$*:Myh11-cre/ERT2* arteries also produced a faint 318 bp band, suggesting that PKD2 is expressed in vascular wall cell types other than myocytes where DNA would not undergo recombination (Figure 1 - figure supplement 1).

PKD2 transcripts and protein are absent in arterial myocytes of tamoxifen-treated *Pkd2*$^{fl/fl}$*:Myh11-cre/ERT2* mice

RT-PCR was performed on RNA extracted from arterial myocytes (~500 cells) that had been individually harvested from mesenteric arteries of tamoxifen-treated *Pkd2*$^{fl/fl}$ and tamoxifen-treated

Pkd2$^{fl/fl}$*:Myh11-cre/ERT2* mice. Arterial myocyte cDNA from both genotypes amplified transcripts for both actin and myosin heavy chain 11, a smooth muscle-specific marker (Figure 1A). In contrast, products for PECAM, an endothelial cell marker, and aquaporin 4, an astrocyte marker, were not amplified, suggesting that the isolated mRNA was from pure smooth muscle (Figure 1A). PKD2 primers were designed to anneal to a sequence in exons 9/10 (forward) and 13 (reverse), which span the recombination site (Figure 1A). Transcripts for PKD2 were amplified by cDNA from arterial myocytes of *Pkd2*$^{fl/fl}$ mice, but not arterial myocytes of *Pkd2*$^{fl/fl}$*:Myh11-cre/ERT2* mice (Figure 1A). These data indicate that tamoxifen induces PKD2 knockout in arterial myocytes of the *Pkd2*$^{fl/fl}$:smCre^{+} mice (Figure 1A).

Western blotting was performed to quantify proteins in intact arteries of tamoxifen-injected *Pkd2*$^{fl/fl}$*:Myh11-cre/ERT2* and tamoxifen-injected *Pkd2*$^{fl/fl}$ mice. In mesenteric and hindlimb arteries of *Pkd2*$^{fl/fl}$*:Myh11-cre/ERT2* mice, PKD2 protein was ~25.3% and 32.6%, respectively of that in *Pkd2*$^{fl/fl}$ controls (Figures 1B, C, figure 1 - figure supplement 2A, B). In contrast, TRPC6, TRPM4, and ANO1 channels and PKD1, which can form a complex with PKD2 [14, 15], were similar between genotypes (Figure 1C, figure 1 - figure supplement 2A, B). $Ca_V1.2$ protein was similar in mesenteric arteries, but slightly higher (~25.6 %) in hindlimb arteries of *Pkd2*$^{fl/fl}$*:Myh11-cre/ERT2* mice (Figures 1B, C, figure 1 – figure supplement B). In aorta of *Pkd2*$^{fl/fl}$*:Myh11-cre/ERT2* mice, PKD2 protein was ~46.8 % of that in *Pkd2*$^{fl/fl}$, whereas $Ca_V1.2$ and PKD1 were similar (Figure 1 – figure supplement 2C and D). Piezo1, angiotensin II type 1 receptors and GPR68 have been proposed to act as vascular mechanosensors ([16-19]). Piezo1, angiotensin II type 1 receptors and GPR68 proteins were similar in mesenteric and hindlimb arteries of *Pkd2*$^{fl/fl}$ and *Pkd2*$^{fl/fl}$*:Myh11-cre/ERT2* mice (Figure 1 - figure supplement 3). α-adrenergic receptor subtypes 1A, 1B and 1D were also measured and all were similar in mesenteric and hindlimb arteries of *Pkd2*$^{fl/fl}$ and *Pkd2*$^{fl/fl}$*:Myh11-cre/ERT2* mice (Figure 1 - figure supplement 3).

Immunofluorescence demonstrated that PKD2 protein was present in myocytes of intact arteries and in isolated myocytes of tamoxifen-treated *Pkd2*$^{fl/fl}$ control mice, but absent in myocytes of tamoxifen-treated *Pkd2*$^{fl/fl}$*:Myh11-cre/ERT2* mice (Figures 1D, E). In contrast, PKD2 protein was present in endothelial cells of both tamoxifen-treated *Pkd2*$^{fl/fl}$ and *Pkd2*$^{fl/fl}$*:Myh11-cre/ERT2* mouse arteries (Figure 1D). These data indicate that PKD2 detected in Western blots of tamoxifen-treated *Pkd2*$^{fl/fl}$*:Myh11-cre/ERT2* mouse arteries is protein present in cell types other than myocytes that would not be targeted by the smooth muscle-specific Cre. These results indicate that PKD2 is expressed in myocytes of mesenteric and hindlimb arteries and aorta and that tamoxifen treatment of *Pkd2*$^{fl/fl}$*:Myh11-cre/ERT2* mice selectively abolishes PKD2 expression in myocytes. From this point in the manuscript,

tamoxifen-treated *Pkd2*$^{fl/fl}$*:Myh11-cre/ERT2* mice will be referred to as *Pkd2* smKO, with tamoxifen-treated *Pkd2*$^{fl/fl}$ mice used as controls in all experiments.

***Pkd2* smKO mice are hypotensive**

Telemetry indicated that diastolic and systolic blood pressures were both lower in *Pkd2* smKO mice than in *Pkd2*$^{fl/fl}$ mice (Figure 2A, 2B). Mean arterial pressure (MAP) was lower in *Pkd2* smKO mice during both day and night cycles, was sustained for days and on average was ~22.5 % lower in *Pkd2* smKO mice than in *Pkd2*$^{fl/fl}$ mice (Figure 2C, figure 2 - figure supplement 1A). Locomotion was similar between genotypes, indicating that the lower blood pressure in *Pkd2* smKO mice was not due to inactivity (Figure 2 - figure supplement 1B). Echocardiography indicated that cardiac output, fractional shortening, ejection fraction and heart rate were similar in *Pkd2* smKO and *Pkd2*$^{fl/fl}$ mice (Figure 2D). *Pkd2* smKO kidney glomeruli and tubules were normal and indistinguishable from those of *Pkd2*$^{fl/fl}$ mice (Figure 2E). Plasma angiotensin II, aldosterone and ANP and plasma and urine electrolytes were similar in *Pkd2* smKO and *Pkd2*$^{fl/fl}$ mice (Table 1, $p>0.05$ for all). These results demonstrate that arterial myocyte PKD2 channels control systemic blood pressure and that cardiac function and kidney anatomy and function are similar in *Pkd2* smKO and *Pkd2*$^{fl/fl}$ mice.

Myocyte PKD2 channels are essential for pressure-induced vasoconstriction in hindlimb arteries

Intravascular pressure stimulates vasoconstriction in small, resistance-size arteries. This myogenic response is a major regulator of both regional organ blood flow and systemic blood pressure. To determine whether PKD2 channels contribute to myogenic tone, pressure-induced (20-100 mmHg) vasoconstriction was measured in first-order gastrocnemius arteries. Intravascular pressures greater than 40 mmHg produced increasing levels of constriction in *Pkd2*$^{fl/fl}$ arteries, reaching ~20.9 % tone at 100 mmHg (Figures 3A, B). In contrast, pressure-induced vasoconstriction was robustly attenuated in *Pkd2* smKO gastrocnemius arteries, which developed only ~5.4 % tone at 100 mmHg or approximately one quarter of that in *Pkd2*$^{fl/fl}$ arteries (Figures 3A, B). The passive diameters of *Pkd2*$^{fl/fl}$ and *Pkd2* smKO gastrocnemius arteries were similar (Figure 3 – figure supplement 1A). Depolarization (60 mM K^+) stimulated slightly larger vasoconstriction in *Pkd2* smKO than *Pkd2*$^{fl/fl}$ gastrocnemius arteries (Figure 3 - figure supplement 1B). These data are consistent with the small increase in $Ca_V1.2$ protein measured in gastrocnemius arteries of *Pkd2* smKO mice and indicate that attenuation of the myogenic response is not due to loss of voltage-dependent Ca^{2+} channel function and that the reduction in systemic blood pressure may stimulate $Ca_V1.2$ expression in hindlimb arteries, but not in mesenteric arteries or aorta (Figure 1C, figure 1 - figure supplement 2B).

Sympathetic control of blood pressure occurs in part due to the activation of α_1-adrenergic receptors in arterial myocytes. To investigate the contribution of myocyte PKD2 channels to α_1-adrenergic receptor-mediated vasoconstriction, responses to phenylephrine, a selective α_1-adrenergic receptor agonist, were measured. Phenylephrine stimulated similar vasoconstrictions in pressurized gastrocnemius arteries of *Pkd2*$^{fl/fl}$ and *Pkd2* smKO mice (Figure 3 – figure supplement 1C). To determine whether this similar response to receptor agonists was specific to α_1-adrenergic receptors, vasoregulation by angiotensin II was measured. Angiotensin II also stimulated similar vasoconstrictions in *Pkd2*$^{fl/fl}$ and *Pkd2* smKO mouse gastrocnemius arteries (Figure 3 - figure supplement 1D). To study vasoregulation in intact skeletal muscle, a perfused hindlimb preparation was used. Stepwise increases in intravascular flow produced lower pressures in hindlimbs of *Pkd2* smKO mice than in those of *Pkd2*$^{fl/fl}$ mice (Figures 3C, D). For example, at a flow rate of at 2.5 ml/min the mean pressure in hindlimbs of *Pkd2* smKO mice were ~63.2 % of those in *Pkd2*$^{fl/fl}$ mice (Figures 3C, D). In contrast, at constant flow, phenylephrine similarly increased pressure in hindlimbs of *Pkd2* smKO and *Pkd2*$^{fl/fl}$ mice (Figure 3 - figure supplement 1E). These data suggest that arterial myocyte PKD2 channels are essential for pressure-induced vasoconstriction, but not phenylephrine- or angiotensin II-induced vasoconstriction, in hindlimb arteries.

Pressure-induced membrane depolarization requires myocyte PKD2 channels in hindlimb arteries

To investigate the mechanism(s) by which myocyte PKD2 channels regulate contractility, membrane potential was measured in pressurized hindlimb arteries using glass microelectrodes. At 10 mmHg, the mean membrane potential of *Pkd2*$^{fl/fl}$ and *Pkd2* smKO arteries were similar at ~ -59.6 and -58.5 mV, respectively (Figure 4A, B). Increasing intravascular pressure to 100 mmHg depolarized *Pkd2*$^{fl/fl}$ arteries by ~22.5 mV, but did not alter the membrane potential of arteries from *Pkd2* smKO mice (Figure 4A, B). In contrast, phenylephrine depolarized arteries to similar membrane potentials in both genotypes (Figure 4A, B). These data suggest that pressure activates PKD2 channels in myocytes of hindlimb arteries, leading to depolarization and vasoconstriction.

Swelling activates PKD2 channels in hindlimb artery myocytes

The contribution of PKD2 channels to mechanosensitive currents was investigated in hindlimb artery myocytes. Recent evidence indicates that recombinant PKD2 generates voltage-dependent, outwardly rectifying currents and is primarily a Na^+-permeant channel under physiological membrane potentials and ionic gradients [7, 20]. Whole cell I_{Cat} was recorded using the whole-cell patch-clamp configuration with symmetrical Na^+ solutions. In *Pkd2*$^{fl/fl}$ myocytes, reducing bath solution osmolarity from 300 to

250 mOsm caused cell swelling and activated an outwardly rectifying I_{Cat} that increased 2.3±0.3- and 3.0±0.7-fold at -100 and +100 mV, respectively ($P<0.05$, n=5, Figure 4C). Swelling-activated I_{Cat} was inhibited by Gd^{3+}, a non-selective cation channel blocker (Figure 4C, D, E). The mean reversal potential for I_{Cat} was similar in isotonic (-0.2±1.3 mV) and hypotonic solutions (0.1±3.8 mV; $P>0.05$), suggesting that swelling activated a I_{Na}. To test this conclusion experimentally, Na^+ substitution experiments were performed. In a hypotonic bath solution, a reduction in bath [Na^+] from 115 to 40 mM shifted the E_{rev} to -14.6±0.5 mV in *Pkd2*$^{fl/fl}$ myocytes (n=5, $P<0.05$ versus E_{rev} in 250 mOsm) (Figure 4F). When adjusted for the liquid junction potential caused by the solution change (+6.9 mV), the corrected E_{rev} is -21.5±0.5 mV, which is similar to the calculated E_{Na} (-24.2 mV). Reducing bath Na^+ also decreased inward current and increased outward current. In contrast, swelling did not activate a I_{Cat} ($P<0.05$, n=5), nor did Gd^{3+} alter I_{Cat} when applied in hypotonic bath solution, in hindlimb artery myocytes of *Pkd2* smKO mice (Figure 4C, D, E). In further contrast to the differential effects of cell swelling, phenylephrine activated similar amplitude I_{Cat}s in hindlimb artery myocytes of *Pkd2*$^{fl/fl}$ and *Pkd2* smKO mice (Figure 4 – figure supplement 1). These data indicate that cell swelling activates PKD2 channels, leading to a Na^+ current in hindlimb artery myocytes, whereas phenylephrine does not activate PKD2 channels in this cell type.

Myocyte PKD2 channels contribute to phenylephrine-induced vasoconstriction in mesenteric arteries

Mesenteric arteries were studied to determine whether myocyte PKD2 channels control contractility in another arterial bed that is a major regulator of systemic blood pressure. In contrast to the robust attenuation of myogenic vasoconstriction in gastrocnemius arteries of *Pkd2* smKO mice, pressure- and depolarization-induced vasoconstriction was similar in mesenteric arteries of *Pkd2* smKO and *Pkd2*$^{fl/fl}$ mice (Figure 5A, figure 5 – figure supplement 1B). Myogenic tone was similar regardless of whether third, fourth, or fifth-order *Pkd2* smKO and *Pkd2*$^{fl/fl}$ mouse mesenteric arteries were studied (Figure 5 - figure supplement 1A). Passive diameter of mesenteric arteries was not altered by myocyte PKD2 knockout (Figure 3 - figure supplement 1A). The differential contribution of myocyte PKD2 channels to pressure-induced vasoconstriction in gastrocnemius and mesenteric arteries was not due to size, as passive diameters of first-order gastrocnemius and third-order mesenteric arteries were similar (Figure 3 supplement 1A).

The splanchnic circulation receives considerable sympathetic innervation. To investigate the contribution of myocyte PKD2 channels to α_1-adrenoceptor-mediated responses, phenylephrine-induced vasoconstriction was measured. Phenylephrine-induced isometric contractions in mesenteric artery (first- and second-order) rings of *Pkd2* smKO mice were smaller than those in *Pkd2*$^{fl/fl}$ controls (Figure

5B, C). For instance, with 1 μM phenylephrine, contractions in *Pkd2* smKO arteries were ~15.3 % of those in *Pkd2*$^{fl/fl}$ arteries, with maximal phenylephrine-induced contraction ~57.3 % of that in *Pkd2*$^{fl/fl}$ arteries (Figure 5B, C). The mean concentration of phenylephrine-induced half-maximal contraction (EC_{50}, μM) was slightly higher in *Pkd2* smKO (2.4±0.2) than *Pkd2*$^{fl/fl}$ (1.1±0.3) arteries (P<0.05, Figure 5B, C). In pressurized (80 mmHg) mesenteric (fourth- and fifth-order) arteries of *Pkd2* smKO mice, phenylephrine-induced vasoconstrictions were between ~50.9 and 64.8 % of those in *Pkd2*$^{fl/fl}$ controls (Figure 5D, E). Similar results were obtained with endothelium-denuded mesenteric arteries, indicating that attenuated vasoconstriction to phenylephrine was due to loss of PKD2 in myocytes (Figure 5 - figure supplement 1C and D). In contrast to attenuated phenylephrine-mediated vasoconstriction, angiotensin II-induced constriction was not different between *Pkd2*$^{fl/fl}$ and *Pkd2* smKO mesenteric arteries (Figure 5 – figure supplement 1E). These data indicate that arterial myocyte PKD2 channels are activated by distinct vasoconstrictor stimuli in arteries of different tissues, contributing to α_1-adrenoceptor-mediated vasoconstriction in mesenteric arteries and essential for the myogenic response in hindlimb arteries.

α_1-adrenergic receptors stimulate myocyte PKD2 channels, leading to membrane depolarization in mesenteric arteries

At an intravascular pressure of 10 mmHg, the membrane potential of *Pkd2*$^{fl/fl}$ and *Pkd2* smKO mesenteric arteries was similar (Figure 6A, B). An increase in pressure to 80 mmHg stimulated a similar depolarization in mesenteric arteries of *Pkd2*$^{fl/fl}$ and *Pkd2* smKO mice, to ~39.7 and 36.7 mV, respectively (Figure 6A, B). Phenylephrine application further depolarized *Pkd2*$^{fl/fl}$ mesenteric arteries by ~19.9 mV, but did not change the membrane potential of *Pkd2* smKO arteries (Figure 6A, B).

To examine phenylephrine-regulation of I_{Cat} in isolated mesenteric artery myocytes, the whole-cell patch-clamp configuration was used with symmetrical 140 mM NaCl. In *Pkd2*$^{fl/fl}$ cells, phenylephrine activated outwardly rectifying I_{Cat}, increasing density ~1.43- and 1.57-fold at -100 mV and +100 mV, respectively (Figure 6C, D). In the presence of phenylephrine, a reduction in bath $[Na]_o$ from 140 to 40 mM shifted the E_{rev} from 0.5±0.5 to -23.2±1.6 mV in *Pkd2*$^{fl/fl}$ myocytes (n=5, P<0.05 versus PE/low Na^+). When corrected for the liquid junction potential (+5.6 mV) caused by the change in bath $[Na]_o$, this E_{rev} is -28.8±1.6 mV, which is similar to calculated E_{Na} (-32.8 mV) under these conditions. Reducing bath Na^+ also reduced inward current and increased outward current. The subsequent addition of Gd^{3+} reduced current density to ~44.9 and 20.7 % of that in phenylephrine/40 mM Na^+at -100 and +100 mV, respectively (n=5, P<0.05, Figure 6C). In contrast to effects in *Pkd2*$^{fl/fl}$ myocytes, phenylephrine did not alter I_{Cat} in *Pkd2* smKO myocytes (Figure 6C, D). In further contrast to

the differential effects of phenylephrine, swelling activated similar amplitude I_{Cat} in mesenteric artery myocytes of *Pkd2*$^{fl/fl}$ and *Pkd2* smKO mice (Figure 6 - figure supplement 1). These data indicate that phenylephrine activates PKD2 channels, leading to a I_{Na} in mesenteric artery myocytes, whereas cell swelling does not activate PKD2 channels in mesenteric artery myocytes.

PKD2 channel knockout in arterial myocytes attenuates hypertension

We tested the hypothesis that arterial myocyte PKD2 channels are associated with the increase in blood pressure during hypertension. Angiotensin II-infusion is a well-established method to produce a stable elevation in mean arterial pressure. Blood pressure was measured following implantation of subcutaneous osmotic minipumps that infused angiotensin II or saline in *Pkd2* smKO and *Pkd2*$^{fl/fl}$ mice. Angiotensin II steadily increased MAP to a plateau of ~155.6 mmHg in *Pkd2*$^{fl/fl}$ mice and to ~134.6 mmHg in *Pkd2* smKO mice (Figure 7A). The angiotensin II-induced increase in MAP (ΔMAP) was ~25.6 % smaller in *Pkd2* smKO than *Pkd2*$^{fl/fl}$ mice (Figure 7A). Saline infusion did not alter blood pressure in either *Pkd2* smKO or *Pkd2*$^{fl/fl}$ mice. These data indicate that myocyte PKD2 channel knockout reduces both the absolute systemic blood pressure and the increase in blood pressure during hypertension.

Hypertension is associated with an upregulation of both total and surface PKD2 proteins in systemic arteries

To investigate mechanisms by which arterial myocyte PKD2 channels may be associated with an increase in blood pressure during hypertension, total and surface proteins were measured in arteries. PKD2 total protein in mesenteric and hindlimb arteries of angiotensin II-induced hypertensive mice were ~149.2 and 143.4 %, respectively, of those in normotensive mice (Figures 7B, C). Arterial biotinylation revealed that surface PKD2 protein in mesenteric and hindlimb arteries of hypertensive mice were also ~150.3 and 145.9 % of those in controls (Figure 7D, E). In contrast, cellular distribution of PKD2 was similar in mesenteric and hindlimb arteries of normotensive and hypertensive mice, with ~85 % of protein located in the plasma membrane (Figures 7F). These data indicate that during hypertension, an increase in total PKD2 protein leads to an increase in the abundance of surface PKD2 channels.

Myocyte-specific PKD2 channel knockout induces vasodilation and prevents arterial remodeling during hypertension

To test the hypothesis that the reduction in systemic blood pressure in *Pkd2* smKO mice during hypertension was due to vasodilation, the contractility of pressurized (80 mmHg) mesenteric arteries was measured using myography. Phenylephrine-induced vasoconstrictions in angiotensin II-treated *Pkd2* smKO mouse arteries were between ~67.6 and 71.1 % of those in $Pkd2^{fl/fl}$ arteries (Figure 8A). In contrast, myogenic tone was similar in arteries of angiotensin II-treated *Pkd2* smKO and $Pkd2^{fl/fl}$ mice (Figure 8B). These results indicate that knockout of arterial myocyte PKD2 channels attenuates phenylephrine-induced vasoconstriction during hypertension. These data also suggest that hypertension does not promote the emergence of a mechanism by which PKD2 channels contribute to the myogenic response in mesenteric arteries.

Hypertension is associated with inward remodeling of vasculature [21]. To investigate the involvement of myocyte PKD2 channels in pathological remodeling, arterial sections from angiotensin II-treated *Pkd2* smKO and $Pkd2^{fl/fl}$ mice were imaged and analyzed. In saline-treated *Pkd2* smKO and $Pkd2^{fl/fl}$ mice, the wall-to-lumen ratio of mesenteric arteries was similar (Figures 8C, D). Angiotensin II infusion increased the artery wall-to-lumen ratio ~2.9-fold in $Pkd2^{fl/fl}$ mice, but only 1.3-fold in *Pkd2* smKO mice, or ~89.6 % less (Figures 8C, D). These data suggest that PKD2 knockout in myocytes attenuates arterial remodeling during hypertension.

Discussion

Previous studies performed *in vitro* have suggested that arterial myocytes express several different TRP channels, but *in vivo* physiological functions of these proteins are unclear. Here, we generated an inducible, smooth muscle-specific knockout of a TRP channel, PKD2, to investigate blood pressure regulation by this protein. We show that tamoxifen-induced, smooth muscle-specific PKD2 knockout dilates resistance-size systemic arteries and reduces blood pressure. Data indicate that heterogeneous vasoconstrictor stimuli activate PKD2 channels in arterial myocytes of different tissues. PKD2 channel activation leads to a I_{Na} in myocytes, which induces membrane depolarization and vasoconstriction. Furthermore, we show that hypertension is associated with an increase in plasma membrane-resident PKD2 channels. PKD2 channel knockout in myocytes of hypertensive mice caused vasodilation, prevented arterial remodeling and lowered systemic blood pressure. In summary, using an inducible, conditional knockout model we show that arterial myocyte PKD2 channels increase physiological

systemic blood pressure. We also show that arterial myocyte PKD2 channels are upregulated during hypertension and genetic knockout reduces high blood pressure.

The regulation of blood pressure by arterial myocyte TRP proteins and involvement in hypertension are poorly understood [2]. This lack of knowledge is due to several primary factors. First, it is unclear which TRP channel family members are expressed and functional in myocytes of resistance-size systemic arteries that control blood pressure. The identification of a TRP channel in blood vessels that do not regulate systemic blood pressure, such as aorta and cerebral arteries, does not necessarily indicate that the same protein is present in arteries that do control blood pressure [2]. Second, TRP channel expression has often been reported in myocytes that had undergone cell culture or in whole vasculature that contains many different cell types. These studies create uncertainty as to which TRP proteins are present specifically in contractile myocytes of resistance-size systemic arteries [2]. Third, the lack of specific modulators of individual TRP channel subfamily members has significantly hampered studies aimed at identifying *in vitro* and *in vivo* functions of these proteins. Fourth, TRP channels are expressed in many different cell types other than arterial myocytes. Blood pressure measurements in global, non-inducible TRP knockout mice generated contrasting results to those anticipated. Myocyte TRPM4 channel activation leads to vasoconstriction in isolated cerebral arteries, but global, constitutive knockout of TRPM4 elevated blood pressure in mice [3, 22]. Arterial myocyte TRPC6 channel activation contributes to myogenic tone in cerebral arteries, but global, constitutive TRPC6 knockout caused vasoconstriction and elevated blood pressure in mice [4]. TRPV4 channel activation in arterial myocytes leads to vasodilation in isolated vessels, but blood pressure in TRPV4$^{-/-}$ mice was the same or lower than controls [5, 6]. Alternative approaches, such as the inducible, cell-specific knockout model developed here, are valuable to advance knowledge of blood pressure regulation by arterial myocyte TRP channels.

Previous studies performed *in vitro* that investigated vasoregulation by PKD2 channels produced a variety of different findings. RNAi-mediated knockdown of PKD2 inhibited swelling-activated non-selective cation currents (I_{Cat}) in rat cerebral artery myocytes and reduced myogenic tone in pressurized cerebral arteries [10]. In contrast, PKD2 siRNA did not alter myogenic tone in mesenteric arteries of wild-type mice, but increased both stretch-activated cation currents and myogenic vasoconstriction in arteries of constitutive, myocyte PKD1 knockout mice [11]. From these results, the authors suggested that myocyte PKD2 channels inhibit mesenteric vasoconstriction [11]. Global knockout of PKD2 is embryonic-lethal in mice due to cardiovascular and renal defects, prohibiting study of the loss of protein in all tissues on vascular function [23, 24]. In global PKD2$^{+/-}$ mice, an increase in actin and myosin expression lead to larger phenylephrine-induced contraction in aorta and mesenteric arteries [12, 13]. Here, using an inducible cell-specific knockout model, we show that swelling, a mechanical stimulus, activates PKD2 currents in

myocytes of skeletal muscle arteries, whereas phenylephrine activates PKD2 currents in myocytes of mesenteric arteries. Regardless of the stimulus involved, PKD2 activation leads to a Na^+ current, membrane depolarization and vasoconstriction in both artery types. PKD2 appears to be the second TRP protein to have been described in in arterial myocytes of skeletal muscle arteries, TRPV1 being the other [25].

Few studies have measured plasma membrane currents through either recombinant PKD2 channels or PKD2 channels expressed in native cell types. PKD2 channels have been observed at the cell surface, with evidence suggesting that PKD1 is required for PKD2 translocation, although the ability of PKD1 to perform this function has been questioned [7 26]. Here, using arterial biotinylation we show that ~85 % of PKD2 protein is located in the plasma membrane in both mesenteric and hindlimb arteries, consistent with our previous data in cerebral arteries [10]. PKD2 ion permeability has also been a matter of debate. Recombinant PKD2 was initially shown to both conduct Ca^{2+} and to be inhibited by Ca^{2+} [26, 27]. To increase surface-trafficking of recombinant PKD2, a recent study generated a chimera by replacing the pore of PKD2-L1, a related channel that readily traffics to the plasma membrane, with the PKD2 channel pore [7]. This channel, which contained the PKD2 channel filter, generated outwardly-rectifying whole cell currents and was more selective for Na^+ and K^+ than Ca^{2+}, with Ca^{2+} only able to permeate in an inward direction [7]. We also show that PKD2 channels in hindlimb and mesenteric artery myocytes are outwardly rectifying and permeant to Na^+. At physiological arterial potentials of ~-60 to -40 mV, PKD2 channel opening would produce an inward Na^+ current, leading to myocyte membrane depolarization and voltage-dependent Ca^{2+} ($Ca_V1.2$) channel activation [28]. The ensuing increase in intracellular Ca^{2+} concentration would stimulate vasoconstriction and an elevation in blood pressure, as observed here. PKD2 channel knockout abolishes the stimulus-induced inward Na^+ current, attenuating depolarization and vasoconstriction.

The splanchnic and skeletal muscle circulations account for up to 35 and 80 (during physical exertion) % of cardiac output, respectively. Changes in arterial contractility within these organs leads to significant modification of total peripheral resistance and systemic blood pressure. We demonstrate that myocyte PKD2 channels regulate contractility in both of these physiologically important circulations. Our data also show that distinct mechanical and chemical stimuli activate PKD2 channels in these arteries to produce vasoconstriction. Intravasulcar pressure stimulates vasoconstriction in resistance-size arteries from a wide variety of tissues. Mice lacking α_1-adrenergic receptors are hypotensive and have reduced vasoconstrictor responses to phenylephrine in mesenteric arteries, highlighting the relevance of this pathway to blood pressure regulation [29]. α_1-adrenergic receptor activation is reported to stimulate vasoconstriction through the release of intracellular Ca^{2+} stores and the activation of voltage-dependent

Ca^{2+} channels and non-selective cation channels ([30-32]). We show that intravascular pressure stimulates PKD2 channels in myocytes of hindlimb arteries, whereas phenylephrine activates PKD2 channels in mesenteric artery myocytes. Stimulus-induced PKD2 channel activation in these arteries leads to vasoconstriction. Surprisingly, we found that myocyte PKD2 channels do not contribute to the myogenic response in mesenteric arteries or to phenylephrine-induced vasoconstriction in hindlimb arteries. Angiotensin II-induced vasoconstriction did not require myocyte PKD2 channels in either hindlimb or mesenteric arteries. These data indicate that stimuli which activate myocyte PKD2 channels are vascular bed-specific, strengthening the concept that the regulation and function of a protein is not homogeneous in the circulation and findings in myocytes of one arterial bed should not simply be translated to other vasculature.

Arteries of diverse organs are exposed to unique environments, including the range of intravascular pressures and the types and concentrations of vasoconstrictor and vasodilator stimuli that regulate contractility. Thus, it would be surprising if the molecular components of intracellular signaling pathways were identical in arterial myocytes of different organs. It was outside of the central aim of this study and beyond scope to determine the differential mechanisms by which pressure and adrenergic receptors activate PKD2 channels in arteries of different organs. Several possibilities exist. Pressure-induced vasoconstriction was described over 100 years ago and yet the mechanosensor, intracellular signal transduction pathways and the ion channels that produce this physiological response are still unresolved [33]. Candidates for the pressure mechanosensor include, one or more proteins that have been proposed in smooth muscle or non-smooth muscle cell types, proteins that have not yet been discovered, elements of the cytoskeleton, or ion channels that act alone, in series or in parallel with other proteins and may be homomultimeric or heteromultimeric proteins. Piezo1, angiotensin II type 1 receptors and GPR68 have been proposed to act as vascular mechanosensors ([16-19]). Importantly, we show here that there is not a singular, homogeneous mechanism that mediates the myogenic response in all artery types, adding additional complexity to this question. It is possible that intravascular pressure mechanosensors are different in hindlimb and mesenteric artery myocytes. If this is the case, the mechanosensor protein(s) present in hindlimb artery myocytes activates PKD2 channels, whereas the mechanosensor(s) in mesenteric artery myocytes does not stimulate PKD2 and vice versa. The intracellular signaling pathways by which pressure and α_1-adrenergic receptors activate PKD2 channels may also not be the same or may couple differently in myocytes of each artery type. Intracellular pathways that transduce the pressure signal to activate ion channels are not resolved, although G_{q11}-coupled phospholipase C (PLC) activation is one candidate [34]. α_1-adrenergic receptors also activate $G_{q/11}$. Thus, if pressure and α_1-adrenergic receptors both stimulate G_{q11}, local or global proximity signaling to PKD2 channels may

underlie differential signaling in each artery type. When considering the molecular identity of the channels that are involved, PKD2 can form both homotetramers and heteromultimers with other channels, including TRPC1 and TRPV4 [26, 35-38]. Whether PKD2 forms homomers or heteromers with other TRP channels in arterial myocytes is unclear, but differential PKD2 channel tetramerization may also underlie the distinct activation of these proteins by pressure and α_1-adrenergic receptors in hindlimb and mesenteric arteries. Other channels, including TRPC6, TRPM4 and ANO1 contribute to the myogenic tone in cerebral arteries, but their relationship to PKD2-mediated responses in mesenteric and hindlimb arteries is unclear [39-41]. Conceivably, other ion channels may signal in series to PKD2, with the proteins involved and the sequence of events differing in mesenteric and hindlimb artery myocytes. Given the large number of unresolved signaling elements and the possible permutations that would require study, it was beyond scope to determine the differential mechanisms by which pressure and adrenergic receptors activate PKD2 channels in arteries of different organs. Future studies should investigate these possibilities.

Having established that myocyte PKD2 channels regulate arterial contractility and systemic blood pressure, we investigated whether hypertension is associated with an alteration in PKD2 expression, surface protein and function. Total and surface PKD2 protein were both higher in mesenteric and hindlimb arteries of hypertensive mice than in normotensive controls, indicating upregulation. PKD2 protein was primarily located in the plasma membrane in arteries of normotensive and hypertensive mice demonstrating that the distribution of channels was unchanged. These data indicate that hypertension is associated with an increase in the amount of PKD2 protein, which traffics to the plasma membrane, thereby increasing surface channel number. Myocyte-specific PKD2 knockout reduced both phenylephrine-induced vasoconstriction and systemic blood pressure and prevented an increase in wall-to-lumen thickness in hypertensive mice. The angiotensin II-induced elevation in blood pressure was smaller in *Pkd2* smKO mice than in *Pkd2*$^{fl/fl}$ controls, supporting the concept that a higher abundance of surface PKD channels in arterial myocytes was associated with vasoconstriction. Our data demonstrate that myocyte PKD2 channels are upregulated during hypertension and that PKD2 targeting reduces vasoconstriction, blood pressure and arterial remodeling during hypertension, eliciting multi-modal benefits.

When considering our findings, a discussion of human diseases that are known to be associated with PKD2 is warranted. Autosomal Dominant Polycystic Kidney Disease (ADPKD) is the most prevalent monogenic human disease worldwide, affecting 1 in 1000 people. ADPKD occurs due to mutations in either PKD1 or PKD2 proteins [42]. Currently, more than 275 human variants in PKD2 have been identified (Autosomal Dominant Polycystic Kidney Disease Mutation Database, Mayo Clinic;

http://pkdb.pkdcure.org). ADPKD is characterized by the appearance of renal cysts, although a significant proportion of patients with apparently normal renal function develop hypertension prior to the development of cysts [42-44]. Here, we show that myocyte PKD2 knockout reduced systemic blood pressure, which is in apparent contrast to the blood pressure increase observed in ADPKD patients. There are several explanations for these differential findings. First, the effects of complete PKD2 abrogation, such as in the knockout studied here, and that of a PKD2 mutation found in an ADPKD patient, on arterial myocyte function may differ. Second, a global PKD2 mutation in an ADPKD patient will alter the function of all cell types in which PKD2 is expressed. Such widespread changes in the physiology of many different cell types could alter arterial myocyte contractility and blood pressure through a variety of mechanisms, leading to net vasoconstriction even if myocyte PKD2 function is also compromised. Third, in ADPKD patients PKD2 mutation is constitutive, whereas here we studied the effects of PKD2 knockout over a three week period in fully developed adult mice. A constitutive PKD2 mutation may modify vascular development and may have chronic effects on myocyte signaling that would not occur in our study. Fourth, the loss of PKD2 function in arterial myocytes of ADPKD patients may attenuate the blood pressure elevation that occurs due to the loss of PKD2 function in other cell types. Future studies should be designed to investigate the effects of PKD2 mutations that occur in ADPKD patients on vascular myocyte function and systemic blood pressure. Our demonstration that myocyte PKD2 channels regulate blood pressure is a step forward to better understanding the significance of this myocyte ion channel in cardiovascular physiology and disease.

In summary, we show that arterial myocyte PKD2 channels are activated by distinct stimuli in arteries of different tissues, increase systemic blood pressure, are upregulated during hypertension and genetic knockout *in vivo* leads to vasodilation and a reduction in both physiological and high blood pressure.

Acknowledgements

This study was supported by NIH/NHLBI grants HL67061, HL133256 and HL137745 to J.H.J, American Heart Association (AHA) Scientist Development Grants to S.B and M.D.M and AHA postdoctoral fellowship to R.H.

508 **Materials and Methods**

509

Key Resources Table				
Reagent type (species) or resource	**Designation**	**Source or reference**	**Identifiers**	**Additional information**
strain, strain background (*Mus musculus*)	*Pkd2$^{fl/fl}$*	John Hopkins PKD Core	PMID 20862291	Mice with *Pkd2* gene flanked by *loxP* regions
strain, strain background (*M. musculus*)	*Myh11-cre/ERT2*	Jackson Laboratories. PMID 18084302	Stock # 019079 RRID:IMSR_JAX:019079	Mice with tamoxifen-inducible Cre recombinase that is expressed under the smooth muscle myosin heavy polipeptide 11 (*Myh11*) promoter.
strain, strain background (*M. musculus*)	*Pkd2$^{fl/fl}$:Myh11-cre/ERT2*	This paper		Mouse line created in-house by mating *Pkd2$^{fl/fl}$* with *Myh11-cre/ERT2*. Mice with inducible smooth muscle-specific deletion of PKD2.
antibody	anti PKD2 (rabbit polyclonal)	Baltimore PKD Core	Rabbit mAB 3374 CT-14/4,	IF 1:200 dilution
antibody	anti PKD2 (mouse monoclonal)	Santa Cruz	Cat. # sc-100415 RRID:AB_1127284	WB 1:100 dilution, IF 1:100 dilution

antibody	anti PKD1 (mouse monoclonal)	Santa Cruz	Cat. # sc-130554 RRID:AB_2163355	WB 1:100 dilution
antibody	anti $Ca_V1.2$ (mouse monoclonal)	UC Davis/NIH NeuroMab	Cat# 73-053. RRID:AB_10672290	WB 1:100 dilution
antibody	anti ANO1 (rabbit monoclonal)	Abcam	Cat. # ab64085 RRID:AB_1143505	WB 1:100 dilution
antibody	anti TRPC6 (rabbit polyclonal)	Abcam	Cat. # ab62461 RRID:AB_956401	WB 1:1000 dilution
antibody	anti TRPM4 (rabbit polyclonal)	Abcam	Cat. # ab106200 RRID:AB_10865760	WB 1:500 dilution
antibody	anti Actin (mouse monoclonal)	Millipore Sigma	Cat. # MAB1501 RRID:AB_2223041	WB 1:5000 dilution
antibody	Alexa 555 secondary antibodies (anti rabbit and anti mouse)	Thermofisher	Cat. # A-21429 (RRID:AB_141761) and # A-31570 (RRID:AB_2536180)	IF 1:400 dilution
other	Nuclear staining (DAPI)	Thermofisher	Cat. # 3571 RRID:AB_2307445	IF 1:1000 dilution
commercial assay or kit	EZ-Link Sulfo-NHS-LC-LC-Biotin	Thermofisher	Cat. # 21338	
commercial assay or kit	EZ-Link Maleimide-PEG2-Biotin	Thermofisher	Cat. # 21901BID	
commercial assay or kit	Mouse Angiotensin II ELISA kit	Elabscience	Cat. # E-EL-M2612	
commercial assay or kit	Mouse Atrial Natriuretic Peptide ELISA kit	Elabscience	Cat. # E-EL-M0166	
commercial assay or kit	Mouse Aldosterone ELISA kit	Mybiosource	Cat. # MBS775626	
chemical compound, drug	Angiotensin II	Sigma-Aldrich	Cat. # A9525	

Animals. All procedures were approved by the Animal Care and Use Committee of the University of Tennessee. *Pkd2*$^{fl/fl}$ mice with *loxP* sites flanking exons 11-13 of the *Pkd2* gene were obtained from the John Hopkins PKD Core. *Pkd2*$^{fl/fl}$ mice were crossed with tamoxifen-inducible smooth muscle-specific Cre mice (*Myh11-cre/ERT2*, Jackson Labs, ref. [36]) to produce *Pkd2*$^{fl/fl}$*:Myh11-cre/ERT2* mice. Male *Pkd2*$^{fl/fl}$*:Myh11-cre/ERT2* or *Pkd2*$^{fl/fl}$ mice (6-10 weeks of age) were injected with tamoxifen (1 mg/ml, i.p.) once per day for 5 days and studied no earlier than 17 days after the last injection. C57BL/6J mice (12 weeks old) were purchased from Jackson Laboratories. Angiotensin II (1.5 ng/g/min) and saline (0.9 NaCl) were infused in mice using subcutaneous osmotic minipumps (Alzet).

Tissue preparation and myocyte isolation. Mice were euthanized with isofluorane (1.5 %) followed by decapitation. First- to fifth-order mesenteric and hindlimb (saphenous, popilital and gastrocnemius) arteries were removed and placed into ice-cold physiological saline solution (PSS) that contained (in mM): 112 NaCl, 6 KCl, 24 $NaHCO_3$, 1.8 $CaCl_2$, 1.2 $MgSO_4$, 1.2 KH_2PO_4 and 10 glucose, gassed with 21% O_2, 5% CO_2 and 74% N_2 to pH 7.4. Arteries were cleaned of adventitial tissue and myocytes dissociated in isolation solution containing (in mM): 55 NaCl, 80 sodium glutamate, 5.6 KCl, 2 $MgCl_2$, 10 HEPES and 10 glucose (pH 7.4, NaOH) using enzymes, as previously described [14].

Genomic PCR. Genomic DNA was isolated from mesenteric and hindlimb arteries using a Purelink Genomic DNA kit (ThermoFisher Scientific). Reaction conditions used are outlined in the Baltimore PKD core center genotyping protocol (http://baltimorepkdcenter.org/mouse/PCR%20Protocol%20for%20Genotyping%20PKD2KO%20and%20PKD2%5Eneo.pdf). Genotyping was performed using a 3-primer strategy, with primers a (5'-CCTTTCCTCTGGTTCTGGGGAG), b (5'-GTTGATGCTTAGCAGATGATGGC) and c (5'-CTGACAGGCACCTACAGAACAGTG) used to identify floxed and deleted alleles.

RT-PCR. Fresh, dissociated mesenteric artery myocytes were manually collected using an enlarged patch pipette under a microscope. Total RNA was extracted from ~500 myocytes using the Absolutely RNA Nanoprep kit (Agilent Technologies, Santa Clara, CA, USA). First-strand cDNA was synthesized from 1–5 ng RNA using SuperScript IV (Invitrogen, Life Technologies). PCR was performed on first-strand cDNA using the following conditions: an initial denaturation at 94°C for 2 min, followed by 40 cycles of denaturation at 94°C for 30 s, annealing at 56°C for 30 s, and extension at 72°C for 1 min. PCR products were separated on 2 % agarose–TEA gels. Primers were used to amplify transcripts of PKD2, aquaporin 4, myosin heavy chain 11, platelet-endothelial cell adhesion molecule 1 (PECAM-1)

and actin (Supplementary file 1). The PKD2 forward primer spanned the junction of exons 9 and 10 and the reverse primer annealed to exon 13.

Western blotting. Proteins were separated on 7.5% SDS-polyacrylamide gels and blotted onto PVDF membranes. Membranes were blocked with 5% milk and incubated with the following primary antibodies: $Ca_V1.2$ (Neuromab), PKD1 and PKD2 (Santa Cruz, sc-100415), ANO1, TRPC6 and TRPM4 (Abcam) and actin (MilliporeSigma) overnight at 4°C. Membranes were washed and incubated with horseradish peroxidase-conjugated secondary antibodies at room temperature. Protein bands were imaged using an Amersham Imager 600 gel imaging system (GE Healthcare) and quantified using ImageJ software.

***En-face* arterial immunofluorescence.** Arteries were cut longitudinally and fixed with 4 % paraformaldehyde in PBS for 1 h. Following a wash in PBS, arteries were permeabilized with 0.2 % Triton X-100, blocked with 5 % goat serum and incubated overnight with PKD2 primary antibody (Rabbit mAB 3374 CT-14/4: Baltimore PKD Center) at 4 ºC. Arteries were then incubated with Alexa Fluor 555 rabbit anti-mouse secondary antibody (1:400; Molecular Probes) and 4',6-diamidino-2-phenylindole, dihydrochloride (DAPI) (1:1000; Thermo Scientific) for 1 hr at room temperature. Segments were washed with PBS, oriented on slides with the endothelial layer downwards and mounted in 80 % glycerol solution. DAPI and Alexa 555 were excited at 350 nm and 555 nm with emission collected at ≤437 nm and ≥555 nm, respectively.

Isolated arterial myocyte immunofluorescence. Myocytes were plated onto poly-L-lysine-coated coverslips, fixed with 3.7 % paraformaldehyde in PBS and permeabilized with 0.1 % Triton X-100. After blocking with 5 % BSA, cells were incubated with mouse monoclonal anti-PKD2 antibody (Santa Cruz) overnight at 4 °C. Slides were then washed and incubated with Alexa Fluor 555 rabbit anti-mouse secondary antibody (Molecular Probes). Secondary antibodies were washed and coverslips mounted onto slides. Images were acquired using a Zeiss 710 (Carl Zeiss) laser-scanning confocal microscope and 40x and 63x oil immersion objectives.

Kidney histology. Kidney sections were stained with H&E and examined by Probetex, Inc (San Antonio, Texas). Briefly, tubules, glomeruli and vasculature were examined for frequency or homogeneity of pathologic abnormalities. These included characteristics of hypercellularity,

hypocellularity, necrosis, apoptosis, matrix accumulation, inflammation, fibrosis and protein droplets. The size and thickness of the cortex, medulla, papilla, glomeruli, tubules and vasculature were also examined.

Telemetric blood pressure measurements. Radiotelemetric transmitters (PA-C10, Data Sciences International) were implanted subcutaneously into anesthetized mice, with the sensing electrode placed in the aorta via the left carotid artery. Seven days later blood pressures were measured using a PhysioTel Digital telemetry platform (Data Sciences International). Dataquest A.R.T. software was used to acquire and analyze data.

Echocardiography. Mice were anesthetized with isofluorane. Ultrasound gel was placed on a hairless area of the chest before and echocardiography performed using a Visual Sonics Vevo 2100 system. Anesthetic depth, heart rate and body temperature were monitored throughout the procedure.

Arterial histology. Arteries were fixed with paraformaldehyde and embedded in paraffin. 5 μm thick sections were cut using a microtome and mounted on slides. Sections were de-paraffinized, blocked in BSA and incubated with H&E. Images were acquired using a transmitted light microscope (Nikon Optiphot-2) and measurements made using Stereo Investigator software (MicrobrightField, Inc.). Wall-to-lumen ratios were calculated as wall thickness/lumen diameter, where the wall (tunica media) thickness and lumen diameter of each section was the averages of four and two equidistant measurements, respectively.

Blood and urine analysis. Retro-orbital blood was drawn from isofluorane-anesthetized mice using a Microvette Capilliary Blood Collection System (Kent Scientific Corporation). Plasma was extracted and angiotensin II (Elabscience), aldosterone (Mybiosource) and atrial natriuretic peptide (Elabscience) concentrations measured using commercially available ELISA kits and an EL800 plate reader (BioTeK). Mice were housed in individual metabolic cages for 72 hours and urine collected for the final 24 hours. Plasma and urine electrolyte concentrations were measured using the MMPC Core at Yale University.

Pressurized artery myography. Experiments were performed using isolated mouse third-, fourth and fifth-order mesenteric arteries and first-order gastrocnemius arteries using PSS gassed with 21% O_2/5% CO_2/74% N_2 (pH 7.4). Arterial segments 1-2 mm in length were cannulated at each end in a perfusion chamber (Living Systems Instrumentation) continuously perfused with PSS and maintained at 37°C. Intravascular pressure was altered using an attached reservoir and monitored using a pressure transducer.

Luminal flow was absent during experiments. Arterial diameter was measured at 1 Hz using a CCD camera attached to a Nikon TS100-F microscope and the automatic edge-detection function of IonWizard software (Ionoptix). Myogenic tone was calculated as: 100 x ($1-D_{active}/D_{passive}$) where D_{active} is active arterial diameter, and $D_{passive}$ is the diameter determined in the presence of Ca^{2+}-free PSS supplemented with 5 mM EGTA).

Perfused hindlimb pressure measurements. Isolated hindlimbs were inserted into a chamber containing gassed PSS (21% O_2/5% CO_2/74% N_2) that was placed on a heating pad to maintain temperature at 37 °C. The femoral artery was cannulated with a similar diameter glass pipette and perfused with gassed PSS at 37°C using a peristaltic pump. Perfusion pressure was measured using a pressure transducer connected to the inflow. The flow rate was increased stepwise from 0 to 2.5 mL/min in 0.25 mL/min steps to generate a response curve. Values were corrected by subtracting the pressure produced by the pipette alone at each flow rate. Prior to measuring responses to phenylephrine, flow rate was adjusted to maintain a constant perfusion pressure of 80 mmHg. Data were recorded and analyzed using IonWizard software (Ionoptix).

Wire myography. Mesenteric artery segments (1st and 2nd order, 2 mm in length) were mounted on tungsten wires in a multi-channel myography system (Danish Myo Technology). Chambers contained PSS that was continuously gassed with 21% O_2/5% CO_2/74% N_2 (pH 7.4). Arterial rings were subjected to a resting tension of 10 mN and allowed to equilibrate prior to experimentation. Responses were measured to increasing concentrations of phenylephrine or 60 mM K^+. Data were acquired and analyzed using LabChart software (ADInstruments).

Pressurized artery membrane potential measurements. Membrane potential was measured by inserting sharp glass microelectrodes (50–90 mΩ) filled with 3 M KCl into the adventitial side of pressurized mesenteric or hindlimb arteries. Membrane potential was recorded using a WPI FD223a amplifier and digitized using a MiniDigi 1A USB interface, pClamp 9.2 software (Axon Instruments) and a personal computer. Criteria for successful intracellular impalements were: (1) a sharp negative deflection in potential on insertion; (2) stable voltage for at least 1 minute after entry; (3) a sharp positive voltage deflection on exit from the recorded cell and (4) a <10% change in tip resistance after the impalement.

Patch-clamp electrophysiology. Isolated arterial myocytes were allowed to adhere to a glass coverslip in a recording chamber. The conventional whole-cell configuration was used to measure non-selective cation currents (I_{cat}) by applying voltage ramps (0.13 mV/ms) between -100 mV and +100 mV from a holding potential of -40 mV. For cell swelling experiments, the pipette solution contained (in mM): Na^+ aspartate 115, mannitol 50, HEPES 10, glucose 10, EGTA 1, NaGTP 0.2, with free Mg^{2+} and Ca^{2+} of 1 mM and 200 nM, respectively (pH 7.2, NaOH). Isotonic (300 mOsm) bath solution contained (in mM): Na^+ aspartate 115, mannitol 50, glucose 10, HEPES 10, $CaCl_2$ 2, $MgCl_2$ 1 (pH 7.4, NaOH). Hypotonic (250 mOsm) bath solution was the same formulation as isotonic bath solution with the exclusion of mannitol (pH 7.4, NaOH). For experiments that measured I_{Cat} regulation by phenylephrine, the bath solution contained (in mM): 140 NaCl, 10 glucose, 10 HEPES, 1 $MgCl_2$, and pH was adjusted to 7.4 with NaOH. Pipette solution contained: 140 NaCl, 10 HEPES, 10 Glucose, 5 EGTA, 1 MgATP, 0.2 NaGTP, and pH was adjusted to 7.2 with NaOH. Total $MgCl_2$ and total $CaCl_2$ were adjusted to give free Mg^{2+} concentrations of 1 mM and free Ca^{2+} of 200 nM. Free Mg^{2+} and Ca^{2+} were calculated using WebmaxC Standard (http://www.stanford.edu/~cpatton/webmaxcS.htm). Na^+ concentration was reduced in bath solutions through equimolar replacement with *N*-methyl-D-glucamine. Liquid junction potentials that occurred due to a reduction in bath Na^+ concentration were measured experimentally and used to correct reversal potential values measured in myocytes during voltage-clamp experiments. Briefly, liquid junction potentials were determined by measuring the immediate shift in voltage that occurred in a patch-clamp pipette containing pipette solution when bath solution containing normal Na^+ concentration was replaced with one containing low Na^+. Currents were recorded using an Axopatch 200B amplifier and Clampex 10.4 (Molecular Devices), digitized at 5 kHz and filtered at 1 kHz. Offline analysis was performed using Clampfit 10.4.

Arterial biotinylation. Procedures used were similar to those previously described [15]. Briefly, arteries were biotinylated with EZ-Link Sulfo-NHS-LC-LC-Biotin and EZ-Link Maleimide-PEG2-Biotin. Unbound biotin was quenched with glycine-PBS, washed with PBS and then homogenized in radioimmunoprecipitation assay (RIPA) buffer. Protein concentration was normalized and biotinylated surface protein was captured by incubating cell lysates with avidin beads (Pierce) at 4°C. Proteins present in biotinylated and non-biotinylated samples were identified using Western blotting.

Statistical analysis. OriginLab and GraphPad InStat software were used for statistical analyses. Values are expressed as mean ± SEM. Student t-test was used for comparing paired and unpaired data from two populations and ANOVA with Student-Newman-Keuls post hoc test used for multiple group

comparisons. P<0.05 was considered significant. Power analysis was performed to verify that the sample size gave a value of >0.8 if *P* was >0.05.

References

1. Nelson MT, Patlak JB, Worley JF and Standen NB. Calcium channels, potassium channels, and voltage dependence of arterial smooth muscle tone. *Am J Physiol*. 1990;259:C3-18.
2. Earley S and Brayden JE. Transient receptor potential channels in the vasculature. *Physiol Rev*. 2015;95:645-690.
3. Mathar I, Vennekens R, Meissner M, Kees F, Van der Mieren G, Camacho Londono JE, Uhl S, Voets T, Hummel B, van den Bergh A, Herijgers P, Nilius B, Flockerzi V, Schweda F and Freichel M. Increased catecholamine secretion contributes to hypertension in TRPM4-deficient mice. *J Clin Invest*. 2010;120:3267-3279.
4. Dietrich A, Mederos YS, Gollasch M, Gross V, Storch U, Dubrovska G, Obst M, Yildirim E, Salanova B, Kalwa H, Essin K, Pinkenburg O, Luft FC, Gudermann T and Birnbaumer L. Increased vascular smooth muscle contractility in TRPC6$^{-/-}$ mice. *Mol Cell Biol*. 2005;25:6980-6989.
5. Nishijima Y, Zheng X, Lund H, Suzuki M, Mattson DL and Zhang DX. Characterization of blood pressure and endothelial function in TRPV4-deficient mice with l-. *Physiol Rep*. 2014;2:e00199.
6. Earley S, Pauyo T, Drapp R, Tavares MJ, Liedtke W and Brayden JE. TRPV4-dependent dilation of peripheral resistance arteries influences arterial pressure. *Am J Physiol Heart Circ Physiol*. 2009;297:H1096-H1102.
7. Shen PS, Yang X, DeCaen PG, Liu X, Bulkley D, Clapham DE and Cao E. The Structure of the Polycystic Kidney Disease Channel PKD2 in Lipid Nanodiscs. *Cell*. 2016;167:763-773.e11.
8. Griffin MD, Torres VE, Grande JP and Kumar R. Vascular expression of polycystin. *J Am Soc Nephrol*. 1997;8:616-626.
9. Torres VE, Cai Y, Chen X, Wu GQ, Geng L, Cleghorn KA, Johnson CM and Somlo S. Vascular expression of polycystin-2. *J Am Soc Nephrol*. 2001;12:1-9.
10. Narayanan D, Bulley S, Leo MD, Burris SK, Gabrick KS, Boop FA and Jaggar JH. Smooth muscle cell transient receptor potential polycystin-2 (TRPP2) channels contribute to the myogenic response in cerebral arteries. *J Physiol*. 2013;591:5031-5046.
11. Sharif-Naeini R, Folgering JH, Bichet D, Duprat F, Lauritzen I, Arhatte M, Jodar M, Dedman A, Chatelain FC, Schulte U, Retailleau K, Loufrani L, Patel A, Sachs F, Delmas P, Peters DJ and Honore E. Polycystin-1 and -2 dosage regulates pressure sensing. *Cell*. 2009;139:587-596.

12. Qian Q, Hunter LW, Du H, Ren Q, Han Y and Sieck GC. $Pkd2^{+/-}$ vascular smooth muscles develop exaggerated vasocontraction in response to phenylephrine stimulation. *J Am Soc Nephrol*. 2007;18:485-493.
13. Du H, Wang X, Wu J and Qian Q. Phenylephrine induces elevated RhoA activation and smooth muscle alpha-actin expression in $Pkd2^{+/-}$ vascular smooth muscle cells. *Hypertens Res*. 2010;33:37-42.
14. Qian F, Germino FJ, Cai Y, Zhang X, Somlo S and Germino GG. PKD1 interacts with PKD2 through a probable coiled-coil domain. *Nat Genet*. 1997;16:179-183.
15. Tsiokas L, Kim E, Arnould T, Sukhatme VP and Walz G. Homo- and heterodimeric interactions between the gene products of PKD1 and PKD2. *Proc Natl Acad Sci U S A*. 1997;94:6965-6970.
16. Li J, Hou B, Tumova S, Muraki K, Bruns A, Ludlow MJ, Sedo A, Hyman AJ, McKeown L, Young RS, Yuldasheva NY, Majeed Y, Wilson LA, Rode B, Bailey MA, Kim HR, Fu Z, Carter DA, Bilton J, Imrie H, Ajuh P, Dear TN, Cubbon RM, Kearney MT, Prasad RK, Evans PC, Ainscough JF and Beech DJ. Piezo1 integration of vascular architecture with physiological force. *Nature*. 2014;515:279-282.
17. Xu J, Mathur J, Vessieres E, Hammack S, Nonomura K, Favre J, Grimaud L, Petrus M, Francisco A, Li J, Lee V, Xiang FL, Mainquist JK, Cahalan SM, Orth AP, Walker JR, Ma S, Lukacs V, Bordone L, Bandell M, Laffitte B, Xu Y, Chien S, Henrion D and Patapoutian A. GPR68 Senses Flow and Is Essential for Vascular Physiology. *Cell*. 2018;173:762-775 e16.
18. Schleifenbaum J, Kassmann M, Szijarto IA, Hercule HC, Tano JY, Weinert S, Heidenreich M, Pathan AR, Anistan YM, Alenina N, Rusch NJ, Bader M, Jentsch TJ and Gollasch M. Stretch-activation of angiotensin II type 1a receptors contributes to the myogenic response of mouse mesenteric and renal arteries. *Circ Res*. 2014;115:263-72.
19. Blodow S, Schneider H, Storch U, Wizemann R, Forst AL, Gudermann T and Mederos y Schnitzler M. Novel role of mechanosensitive AT1B receptors in myogenic vasoconstriction. *Pflugers Arch*. 2014;466:1343-53.
20. Gonzalez-Perrett S, Batelli M, Kim K, Essafi M, Timpanaro G, Moltabetti N, Reisin IL, Arnaout MA and Cantiello HF. Voltage dependence and pH regulation of human polycystin-2-mediated cation channel activity. *The Journal of biological chemistry*. 2002;277:24959-66.
21. Schiffrin EL. Vascular Remodeling in Hypertension. *Hypertension*. 2012;59:8.
22. Earley S, Waldron BJ and Brayden JE. Critical role for transient receptor potential channel TRPM4 in myogenic constriction of cerebral arteries. *Circ Res*. 2004;95:922-929.

739 23. Wu G, Markowitz GS, Li L, D'Agati VD, Factor SM, Geng L, Tibara S, Tuchman J, Cai Y, Park
740 JH, van AJ, Hou H, Jr., Kucherlapati R, Edelmann W and Somlo S. Cardiac defects and renal failure in
741 mice with targeted mutations in Pkd2. *Nat Genet*. 2000;24:75-78.
742 24. Boulter C, Mulroy S, Webb S, Fleming S, Brindle K and Sandford R. Cardiovascular, skeletal,
743 and renal defects in mice with a targeted disruption of the Pkd1 gene. *Proc Natl Acad Sci U S A*.
744 2001;98:12174-12179.
745 25. Kark T, Bagi Z, Lizanecz E, Pasztor ET, Erdei N, Czikora A, Papp Z, Edes I, Porszasz R and
746 Toth A. Tissue-specific regulation of microvascular diameter: opposite functional roles of neuronal and
747 smooth muscle located vanilloid receptor-1. *Molecular pharmacology*. 2008;73:1405-12.
748 26. Hanaoka K, Qian F, Boletta A, Bhunia AK, Piontek K, Tsiokas L, Sukhatme VP, Guggino WB
749 and Germino GG. Co-assembly of polycystin-1 and -2 produces unique cation-permeable currents.
750 *Nature*. 2000;408:990-994.
751 27. Cai Y, Anyatonwu G, Okuhara D, Lee KB, Yu Z, Onoe T, Mei CL, Qian Q, Geng L, Wiztgall R,
752 Ehrlich BE and Somlo S. Calcium dependence of polycystin-2 channel activity is modulated by
753 phosphorylation at Ser812. *J Biol Chem*. 2004;279:19987-95.
754 28. Jaggar JH, Porter VA, Lederer WJ and Nelson MT. Calcium sparks in smooth muscle. *Am J*
755 *Physiol*. 2000;278:C235-C256.
756 29. Tanoue A, Nasa Y, Koshimizu T, Shinoura H, Oshikawa S, Kawai T, Sunada S, Takeo S and
757 Tsujimoto G. The $alpha_{1D}$-adrenergic receptor directly regulates arterial blood pressure via
758 vasoconstriction. *The Journal of clinical investigation*. 2002;109:765-75.
759 30. Utz J, Eckert R and Trautwein W. Changes of intracellular calcium concentrations by
760 phenylephrine in renal arterial smooth muscle cells. *Pflugers Arch*. 1999;438:7.
761 31. Inoue R and Kuriyama H. Dual regulation of cation-selective channels by muscarinic and alpha
762 1-adrenergic receptors in the rabbit portal vein. *J Physiol*. 1993;465:22.
763 32. Eckert R, Karsten A, Utz J and Ziegler M. Regulation of renal artery smooth muscle tone by
764 alpha1-adrenoceptors: role of voltage-gated calcium channels and intracellular calcium stores. *Urol Res*.
765 2000;28:6.
766 33. Bayliss WM. On the local reactions of the arterial wall to changes in internal pressure. *J Physiol*.
767 1902;28:220-231.
768 34. Kauffenstein G, Laher I, Matrougui K, Guerineau NC and Henrion D. Emerging role of G
769 protein-coupled receptors in microvascular myogenic tone. *Cardiovascular research*. 2012;95:223-32.
770 35. Kottgen M, Buchholz B, Garcia-Gonzalez MA, Kotsis F, Fu X, Doerken M, Boehlke C, Steffl D,
771 Tauber R, Wegierski T, Nitschke R, Suzuki M, Kramer-Zucker A, Germino GG, Watnick T, Prenen J,

Nilius B, Kuehn EW and Walz G. TRPP2 and TRPV4 form a polymodal sensory channel complex. *J Cell Biol*. 2008;182:437-447.

36. Zhang P, Luo Y, Chasan B, Gonzalez-Perrett S, Montalbetti N, Timpanaro GA, Cantero MR, Ramos AJ, Goldmann WH, Zhou J and Cantiello HF. The multimeric structure of polycystin-2 (TRPP2): structural-functional correlates of homo- and hetero-multimers with TRPC1. *Hum Mol Genet*. 2009;18:1238-1251.

37. Bai CX, Giamarchi A, Rodat-Despoix L, Padilla F, Downs T, Tsiokas L and Delmas P. Formation of a new receptor-operated channel by heteromeric assembly of TRPP2 and TRPC1 subunits. *EMBO Rep*. 2008;9:472-479.

38. Gonzalez-Perrett S, Kim K, Ibarra C, Damiano AE, Zotta E, Batelli M, Harris PC, Reisin IL, Arnaout MA and Cantiello HF. Polycystin-2, the protein mutated in autosomal dominant polycystic kidney disease (ADPKD), is a Ca^{2+}-permeable nonselective cation channel. *Proc Natl Acad Sci U S A*. 2001;98:1182-1187.

39. Welsh DG, Morielli AD, Nelson MT and Brayden JE. Transient receptor potential channels regulate myogenic tone of resistance arteries. *Circ Res*. 2002;90:248-250.

40. Earley S, Waldron BJ and Brayden JE. Critical role for transient receptor potential channel TRPM4 in myogenic constriction of cerebral arteries. *Circ Res*. 2004;95:922-929.

41. Bulley S, Neeb ZP, Burris SK, Bannister JP, Thomas-Gatewood CM, Jangsangthong W and Jaggar JH. TMEM16A/ANO1 channels contribute to the myogenic response in cerebral arteries. *Circ Res*. 2012;111:1027-1036.

42. Torres VE, Harris PC and Pirson Y. Autosomal dominant polycystic kidney disease. *Lancet*. 2007;369:1287-1301.

43. Valero FA, Martinez-Vea A, Bardaji A, Gutierrez C, Garcia C, Richart C and Oliver JA. Ambulatory blood pressure and left ventricular mass in normotensive patients with autosomal dominant polycystic kidney disease. *J Am Soc Nephrol*. 1999;10:1020-6.

44. Martinez-Vea A, Bardaj A, Gutierrez C, Garca C, Peralta C, Marcas L and Oliver JA. Exercise blood pressure, cardiac structure, and diastolic function in young normotensive patients with polycystic kidney disease: a prehypertensive state. *American journal of kidney diseases : the official journal of the National Kidney Foundation*. 2004;44:216-23.

	Pkd2$^{fl/fl}$	*Pkd2* smKO
Plasma hormones (pg/ml)		
Angiotensin II	202.5±17.2 (n=16)	204.7±12.1 (n=15)
Aldosterone	341.0±18.2 (n=16)	365.6±14.0 (n=10)
ANP	107.2±9.4 (n=18)	118.3±12.3 (n=18)
Plasma electrolytes (mM)		
Na^+	142.3±1.0 (n=7)	152.0±5.5 (n=6)
K^+	6.4±0.4 (n=7)	6.8±0.3 (n=6)
Cl^-	78.8±0.7 (n=7)	84.1±4.3 (n=6)
Urine electrolytes (mM)		
Na^+	136.9±9.3 (n=15)	147.0±16.2 (n=15)
K^+	563.2±30.2 (n=15)	548.6±37.6 (n=15)
Cl^-	455.4±24.7 (n=15)	479.1±42.0 (n=15)

Table 1. Plasma hormones and plasma and urine electrolytes.

Legend

Supplementary file 1. Primers used for RT PCR. The PKD2 forward primer recognizes nucleotides in exon 9 and 10 and the reverse primer was aligned with a sequence in exon 13.

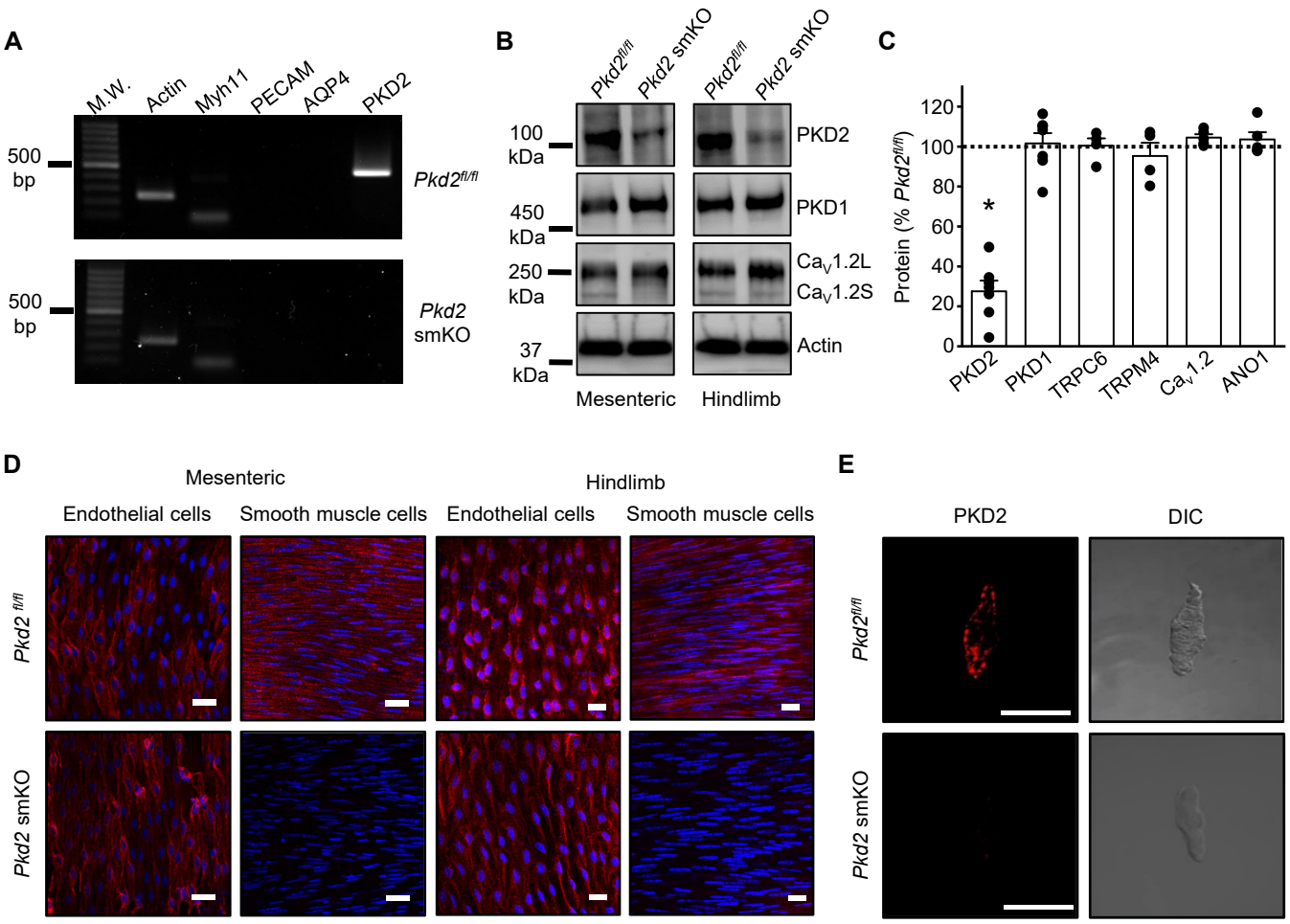

Figure 1: Activation of Cre recombinase abolishes PKD2 in arterial myocytes of *Pkd2$^{fl/fl}$:myh11-cre/ERT2* **mice.** **A.** RT-PCR showing the absence of PKD2 transcript in isolated myocytes from tamoxifen-treated *Pkd2$^{fl/fl}$:myh11-cre/ERT2* mice**. B**: Western blots illustrating the effect of tamoxifen-treatment in *Pkd2$^{fl/fl}$* and *Pkd2$^{fl/fl}$:myh11-cre/ERT2* mice on PKD2, Cav1.2L (full-length Cav1.2) and Cav1.2S (short Cav1.2) proteins in mesenteric and hindlimb arteries. **C**: Mean data for proteins in mesenteric arteries of tamoxifen-treated *Pkd2$^{fl/fl}$:myh11-cre/ERT2* mice when compared to those in tamoxifen-treated *Pkd2$^{fl/fl}$* mice. n=4-7. * indicates $p<0.05$ versus *Pkd2$^{fl/fl}$*. **D**: *En-face* immunofluorescence imaging illustrating that PKD2 protein (red, Alexa Fluor 555) is abolished in myocytes of mesenteric and hindlimb arteries in tamoxifen-treated *Pkd2$^{fl/fl}$:myh11-cre/ERT2* mice (representative of 6 mesenteric and 6 hindlimb arteries). In contrast, PKD2 protein in endothelial cells is unaltered. Nuclear staining (DAPI) is also shown. Scale bars = 20 μm. **E**: Confocal and DIC images illustrating that PKD2 protein (Alexa Fluor 555) is abolished in isolated mesenteric artery myocytes of tamoxifen-treated *Pkd2$^{fl/fl}$:myh11-cre/ERT2* mice (representative data from 5 *Pkd2$^{fl/fl}$* and 5 *Pkd2$^{fl/fl}$:myh11-cre/ERT2* mice). Scale bars = 10 μm.

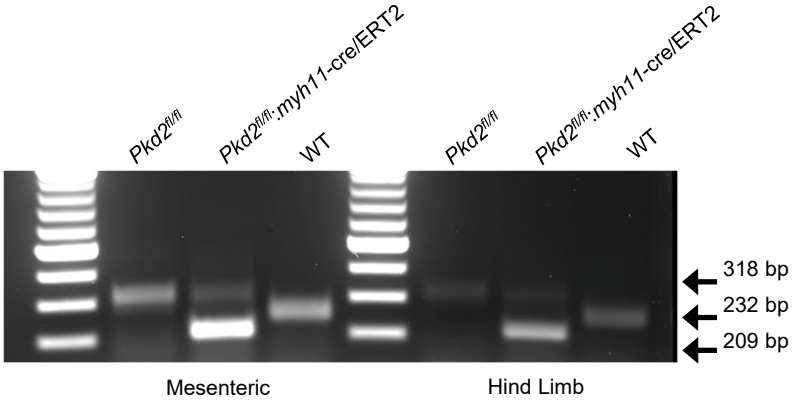

Figure 1 – figure supplement 1 Genotyping of mouse lines. Ethidium bromide gel illustrating PCR products in vasculature of C57BL/6J (WT) mice and tamoxifen-treated *Pkd2*$^{fl/fl}$ and *Pkd2*$^{fl/fl}$*:myh11-cre/ERT2* mice.

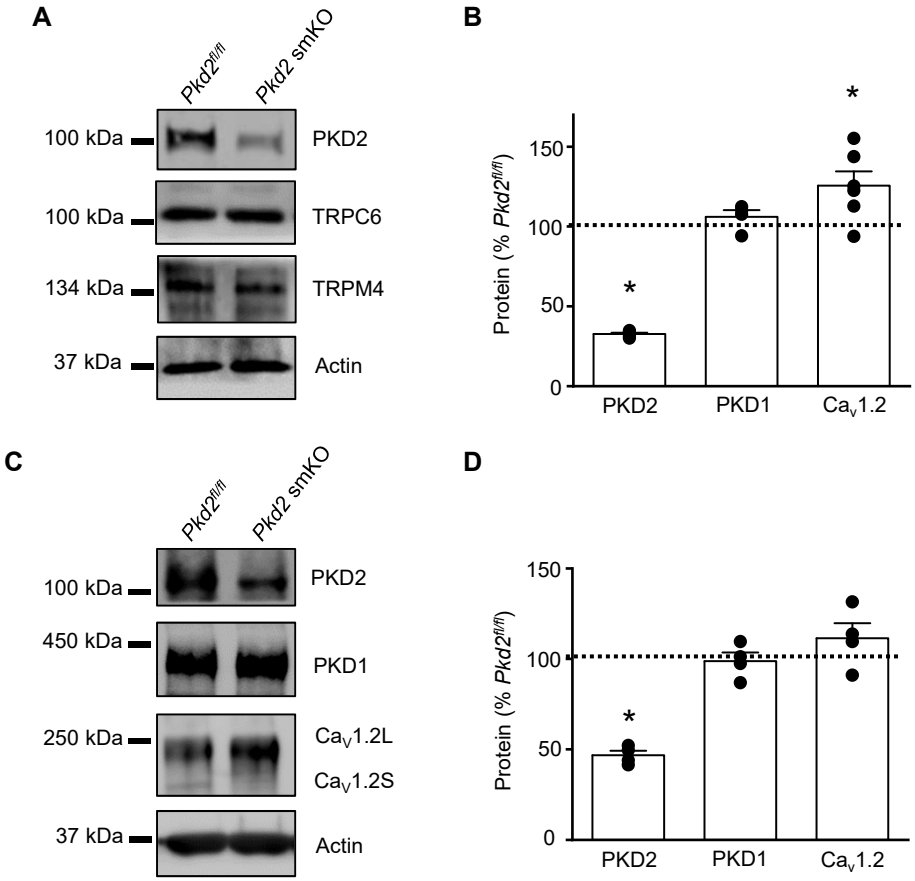

Figure 1 – figure supplement 2: PKD2 protein is lower in aorta and mesenteric and hindlimb arteries from tamoxifen-treated *Pkd2$^{fl/fl}$:myh11-cre/ERT2* mice. A: Western blots illustrating PKD2 protein was lower in mesenteric arteries of tamoxifen-treated *Pkd2$^{fl/fl}$:myh11-cre/ERT2* mice, whereas other proteins were similar. **B**: Mean data for proteins in hindlimb arteries of *Pkd2* smKO mice (n=4-6). **C**: Western blots of proteins in aorta. $Ca_V1.2L$, full-length $Ca_V1.2$; $Ca_V1.2S$, short $Ca_V1.2$. **D**: Mean data from aorta (n=4). * indicates $p<0.05$ versus *Pkd2$^{fl/fl}$*.

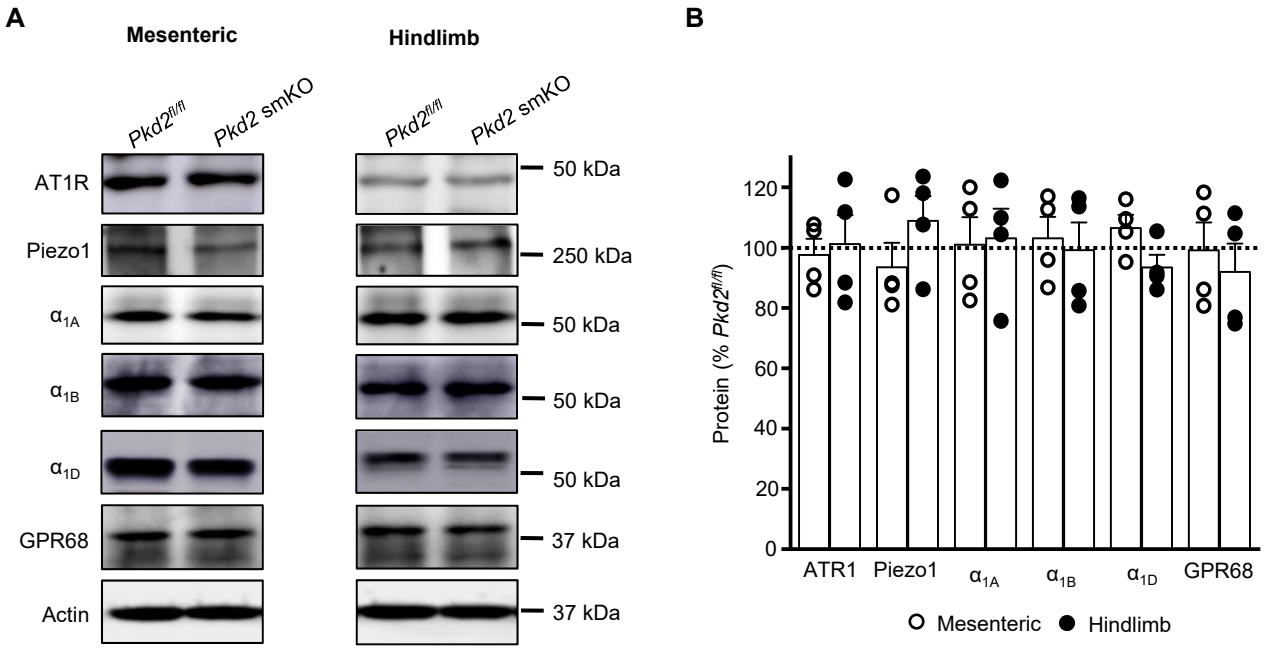

Figure 1 – figure supplement 3: Several proteins that regulate arterial contractility are unchanged in tamoxifen-treated *Pkd2$^{fl/fl}$:myh11-cre/ERT2* mice. A: Western blots illustrating Angiotensin II type 1 receptor (AT1R), Piezo1, α_1-adrenergic receptor A (α_{1A}), α_1-adrenergic receptor B (α_{1B}), α_1-adrenergic receptor D (α_{1D}) and G protein-coupled receptor 68 (GPR68) protein levels in mesenteric and hindlimb arteries of *Pkd2$^{fl/fl}$* and *Pkd2$^{fl/fl}$:myh11-cre/ERT2* mice. **B**: Mean data from mesenteric and hindlimb arteries (n=4 per group).

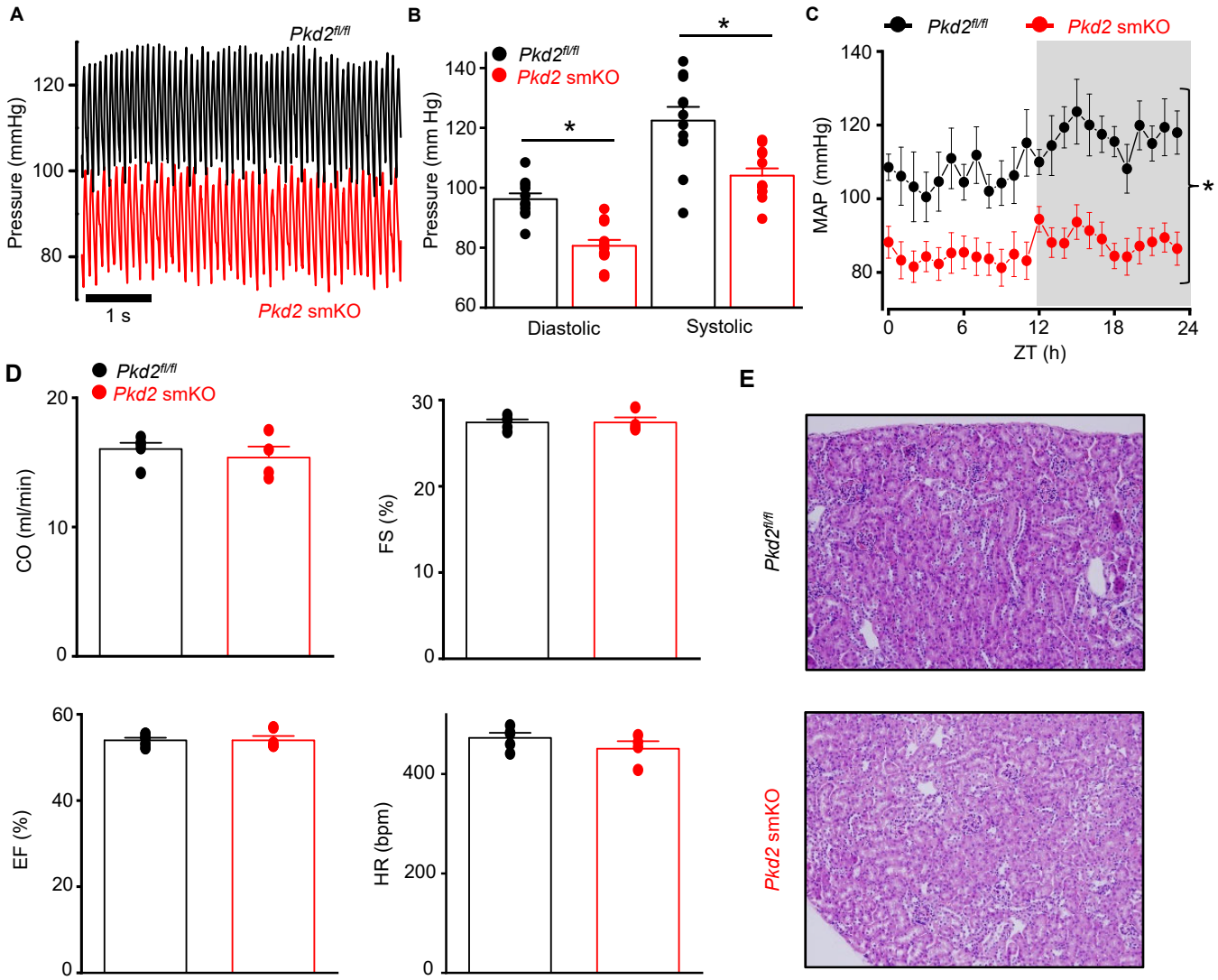

Figure 2: *Pkd2* smKO mice are hypotensive with normal cardiac function and renal histology.

A: Original telemetric blood pressure recordings from *Pkd2* smKO and *Pkd2*$^{fl/fl}$ mice. **B**: Mean systolic and diastolic blood pressures in *Pkd2*$^{fl/fl}$ (n=11) and *Pkd2* smKO (n=12) mice. * indicates $p<0.05$ versus *Pkd2*$^{fl/fl}$. **C**: Mean arterial blood pressures (MAP) in *Pkd2*$^{fl/fl}$ (n=11) and *Pkd2* smKO (n=12) mice during day and night (gray) cycles. ZT: Zeitgeber Time. * indicates $p<0.05$ versus *Pkd2*$^{fl/fl}$ for all data points. **D**: Mean echocardiography data. Cardiac output (CO), fractional shortening (FS), ejection fraction (EF) and heart rate (HR). (*Pkd2*$^{fl/fl}$, n=5; *Pkd2* smKO mice, n=4). **E**: Representative images of H&E stained kidney cortex used for histological assessment (n=3 mice used for for each group).

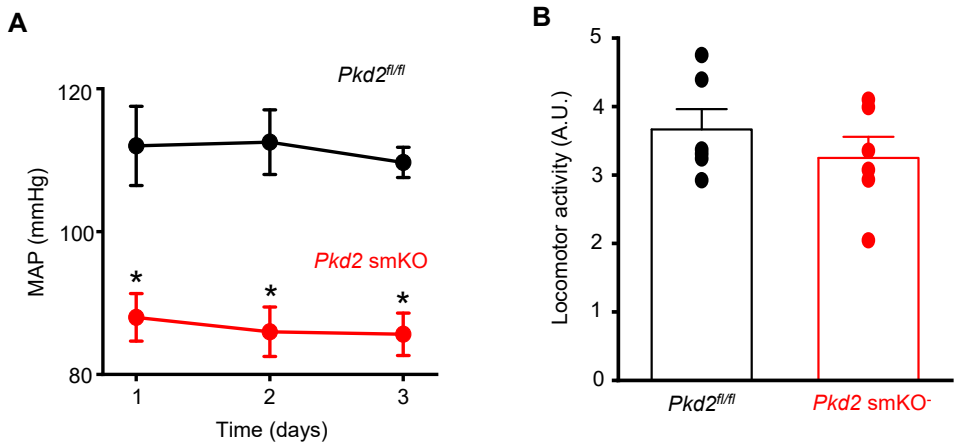

Figure 2 - figure supplement 1: Lower blood pressure is sustained in *Pkd2* smKO mice. A: Mean arterial blood pressure (MAP) in *Pkd2* smKO and *Pkd2*$^{fl/fl}$ mice (n=6 per group). * indicates P<0.05 versus *Pkd2*$^{fl/fl}$. **B:** Mean data of locomotor activity, n=6 per group.

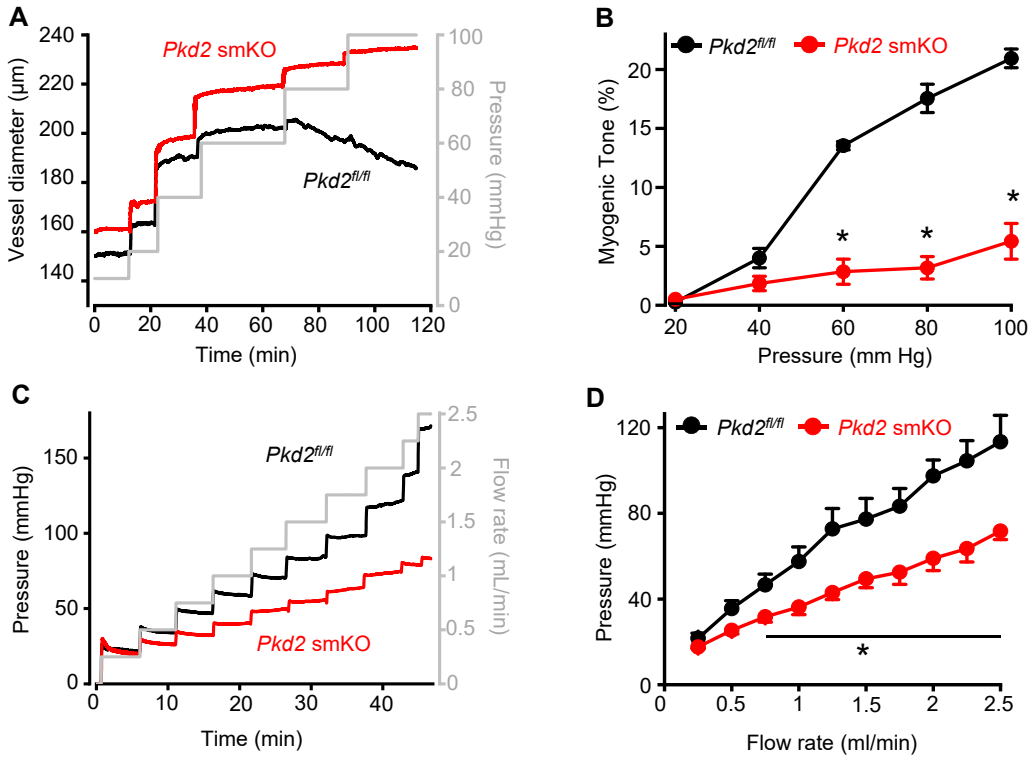

Figure 3: Pressure-induced vasoconstriction is attenuated in *Pkd2* smKO mouse hindlimb arteries. A: Representative traces illustrating diameter responses to intravascular pressure in gastrocnemius arteries of *Pkd2*$^{fl/fl}$ and *Pkd2* smKO mice. **B**: Mean data for myogenic tone in gastrocnemius arteries (*Pkd2*$^{fl/fl}$, n=5; *Pkd2* smKO, n=6). * indicates P<0.05 versus *Pkd2*$^{fl/fl}$. **C**: Representative traces illustrating hindlimb perfusion pressure in response to increasing flow. **D**: Mean data for hindlimb perfusion pressure (*Pkd2*$^{fl/fl}$, n=6; *Pkd2* smKO, n=4). * indicates P<0.05 versus *Pkd2*$^{fl/fl}$.

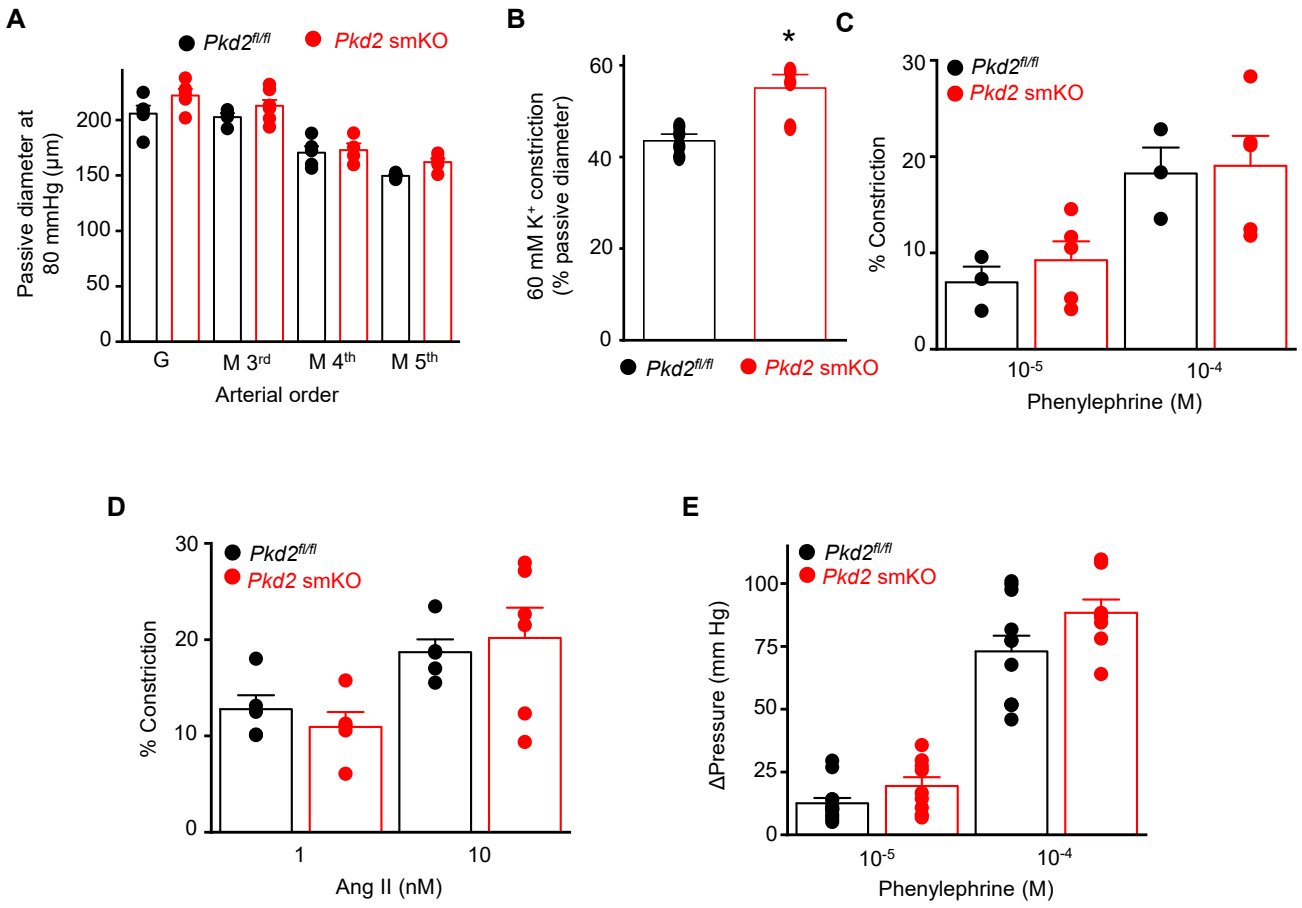

Figure 3 - figure supplement 1: Myocyte PKD2 knockout does not alter phenylephrine or angiotensin II-induced vasoconstriction in hindlimb arteries. A: Mean passive diameter at 80 mmHg of first-order gastrocnemius arteries (G) and third-, fourth- and fifth-order mesenteric arteries (M) (*Pkd2*$^{fl/fl}$: G, n= 5; M3rd n=4; M4th n=5; M5th n=5 and *Pkd2* smKO: G, n= 5; M3rd n=7; M4th n=4; M5th n=5). **B:** Mean data for 60 mM K^+-induced constriction in pressurized (100 mmHg) gastrocnemius arteries from *Pkd2*$^{fl/fl}$ (n=4) and *Pkd2* smKO (n=4) mice. * indicates P<0.05 versus *Pkd2*$^{fl/fl}$. **C:** Mean data of phenylephrine-induced constriction in pressurized gastrocnemius arteries (*Pkd2*$^{fl/fl}$ n= 4, *Pkd2* smKO n=5). **D**: Mean data of angiotensin II-induced constriction in gastrocnemius arteries pressurized to 100 mmHg (*Pkd2*$^{fl/fl}$, n=5 and *Pkd2* smKO, n=5-6). **E**: Mean data of phenylephrine-induced pressure responses in intact hindlimb (*Pkd2*$^{fl/fl}$, n=11-13 and *Pkd2* smKO, n=8-9).

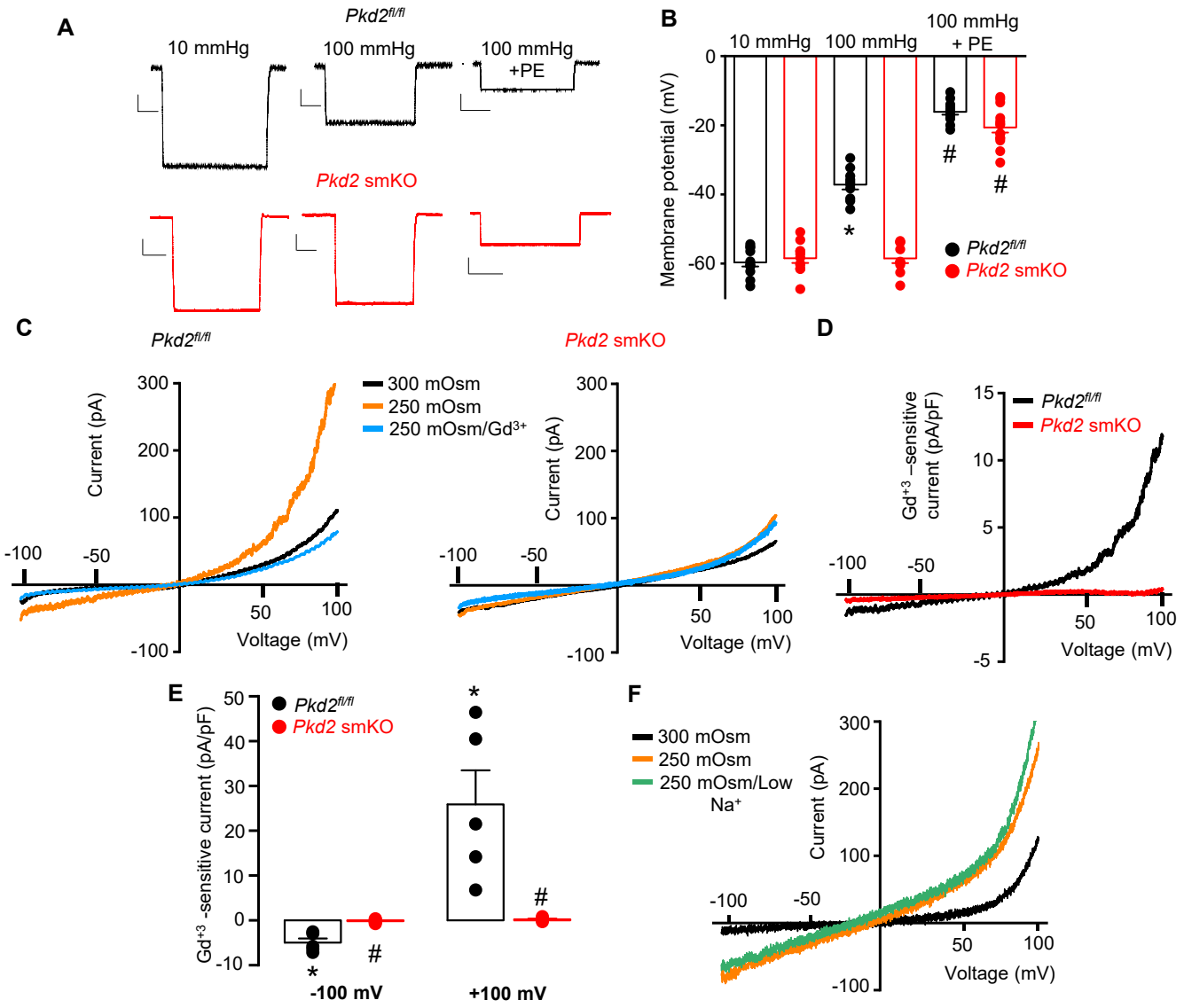

Figure 4: PKD2 channels contribute to pressure-induced hindlimb artery depolarization and swelling-activated Na^+ currents in hindlimb artery myocytes. A: Representative traces of microelectrode impalements under indicated conditions illustrating that pressure-induced depolarization is attenuated in gastrocnemius arteries of *Pkd2* smKO mice. Phenylephrine (PE) = 1 μM. Scale bars: Y= 10 mV, X=20 s. **B:** Mean data for membrane potential recordings in pressurized hindlimb arteries in the absence or presence of PE (*Pkd2*$^{fl/fl}$: 10 mmHg, n=11; 100 mmHg, n=10; 100 mmHg+PE, n=13 and *Pkd2* smKO: 10 mmHg, n=11; 100 mmHg, n=10; 100 mmHg+PE, n=14). * indicates $p<0.05$ versus 10 mmHg in *Pkd2*$^{fl/fl}$. # indicates $p<0.05$ versus 100 mmHg in the same genotype. **C**: Representative I_{Cat}s recorded between -100 and +100 mV in isotonic (300 mOsm), hypotonic (250 mOsm) and hypotonic bath solution with Gd^{3+} (100 μM) in the same *Pkd2*$^{fl/fl}$ and *Pkd2* smKO mouse hindlimb artery myocytes. **D:** Representative I-V relationships of Gd^{+3} -sensitive I_{cat}s activated by hypotonic solution in *Pkd2*$^{fl/fl}$ and *Pkd2* smKO hindlimb myocytes. **E**: Mean data for Gd^{3+}-sensitive I_{Cat}s recorded in hypotonic solution in *Pkd2*$^{fl/fl}$ and *Pkd2* smKO myocytes (n=5 for each). * indicates $p<0.05$ versus 250 mOsm, # $p<0.05$ versus *Pkd2*$^{fl/fl}$. **F:** Representative I-V relationships between -100 and +100 mV in isotonic (300 mOsm), hypotonic (250 mOsm) and hypotonic bath solution with low (40 mM) Na^+ in the same *Pkd2*$^{fl/fl}$ mouse hindlimb artery myocyte.

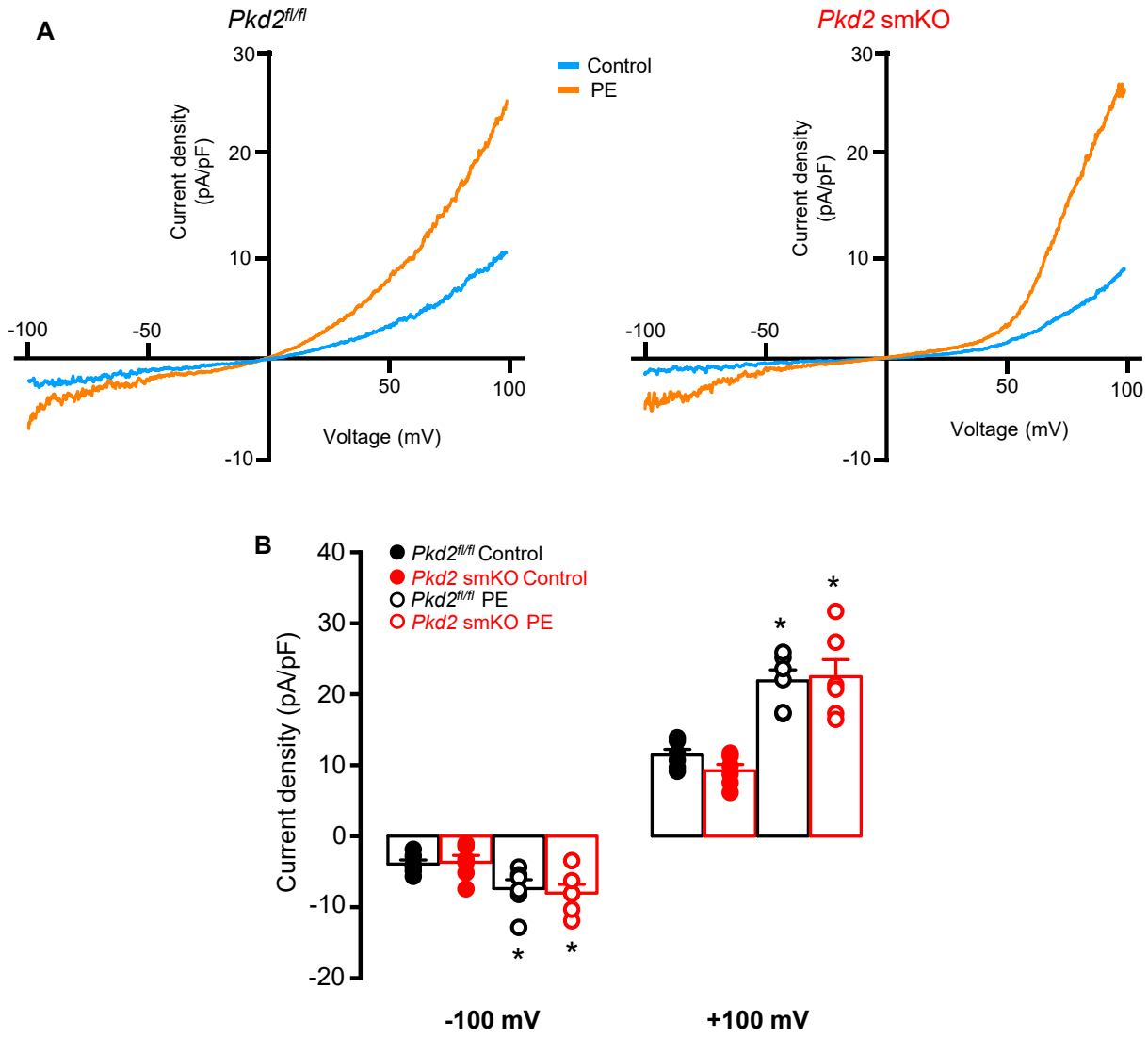

Figure 4 - figure supplement 1: PKD2 knockout does not alter phenylephrine (PE)-activated I_{Cat} in isolated hindlimb artery myocytes A: Representative I-V relationships recorded between -100 and +100 mV in the same hindlimb artery myocytes of *Pkd2*$^{fl/fl}$ or *Pkd2* smKO mice in control and PE (10 μM). **B**: Mean data for current density at -100 and +100 mV (*Pkd2*$^{fl/fl}$, n=6 and *Pkd2* smKO, n=6). * indicates $p<0.05$ versus control in the same genotype.

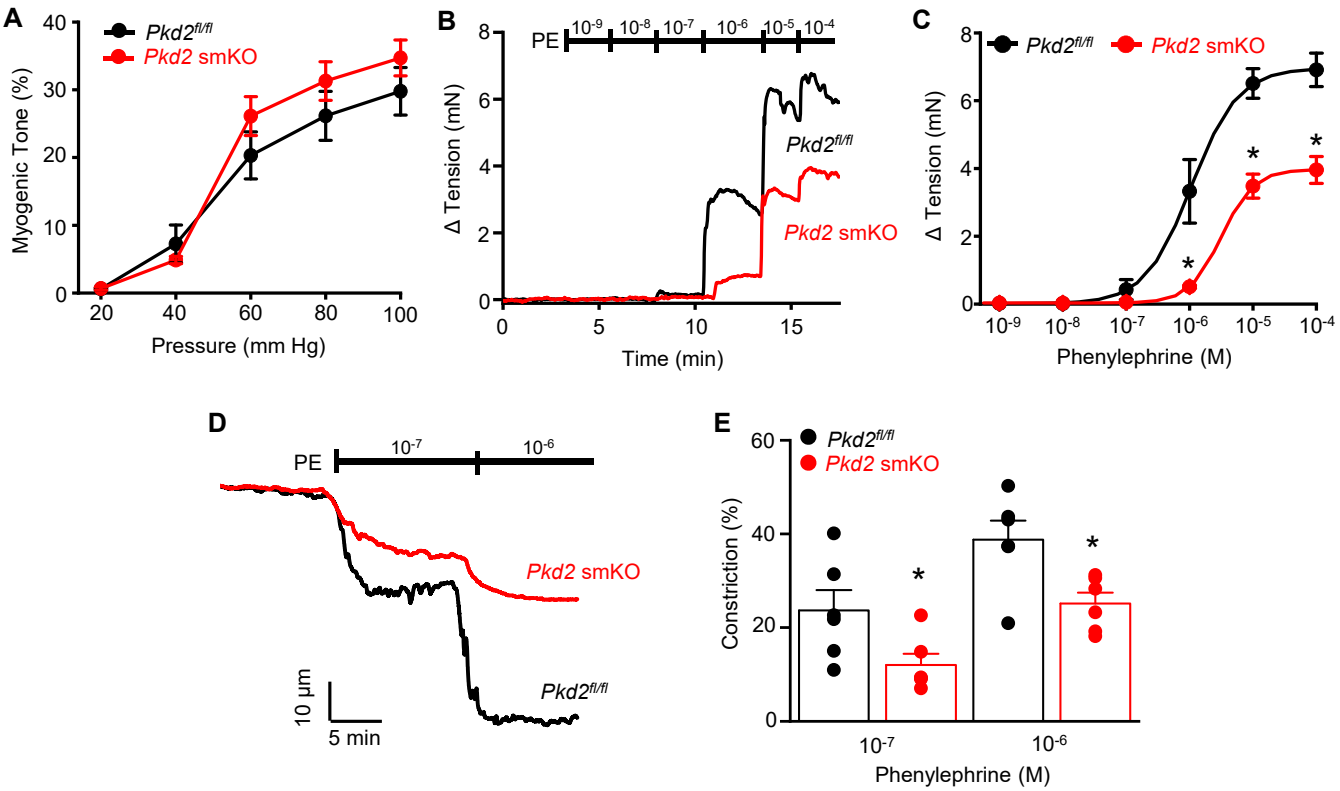

Figure 5: Pressure-induced vasoconstriction is unaltered, whereas phenylephrine-induced vasoconstriction is attenuated, in mesenteric arteries of *Pkd2* smKO mice. A: Mean vasoconstriction over a range of pressures in resistance-size mesenteric arteries from *Pkd2*$^{fl/fl}$ (n=7) and *Pkd2* smKO (n=9) mice. **B**: Original recordings of concentration-dependent, phenylephrine (PE)-induced contraction in mesenteric artery rings. **C**: Mean PE-induced contraction (*Pkd2*$^{fl/fl}$, n=5; *Pkd2* smKO, n=6; * P<0.05 versus *Pkd2*$^{fl/fl}$). **D**: Representative phenylephrine-induced vasoconstriction in pressurized (80 mmHg) fifth-order mesenteric arteries. **E**: Mean PE-induced vasoconstriction in pressurized (80 mmHg) fourth- and fifth-order mesenteric arteries (*Pkd2*$^{fl/fl}$, n=6; *Pkd2* smKO, n=6; * P<0.05 versus *Pkd2*$^{fl/fl}$ at the same PE concentration).

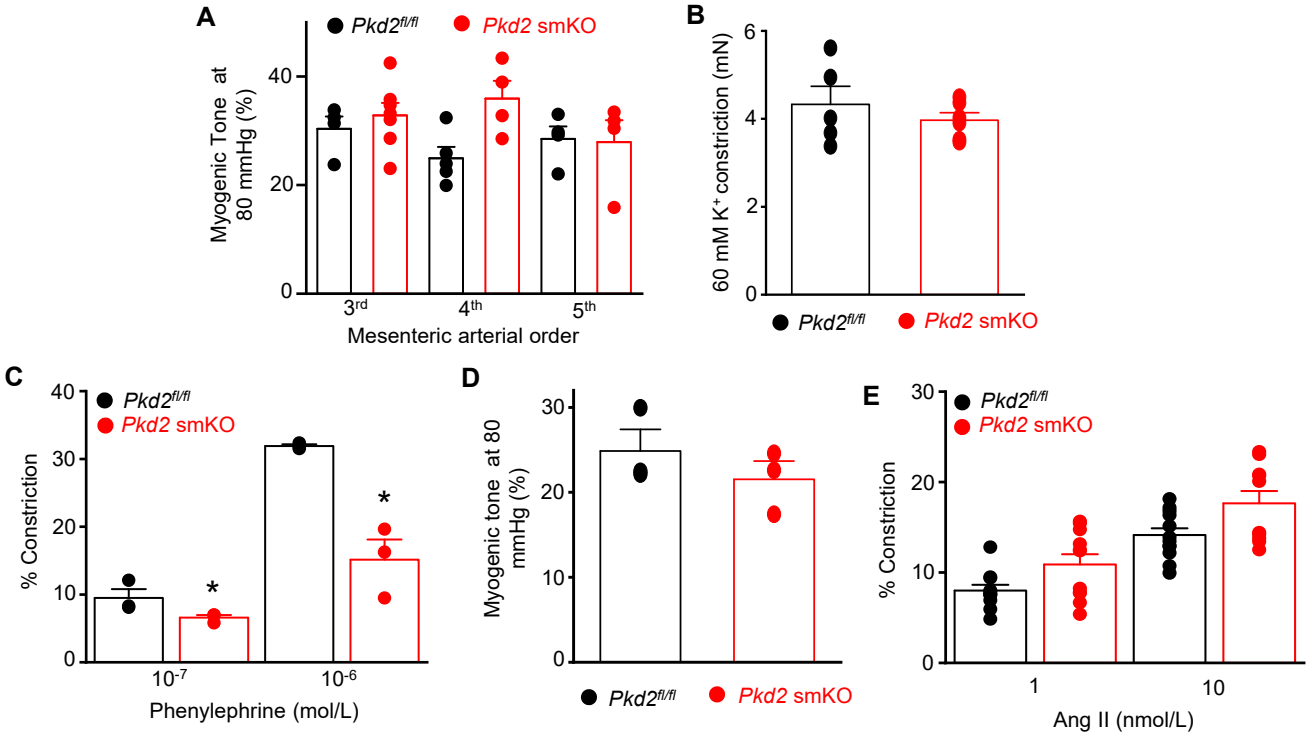

Figure 5 – figure supplement 1: Myocyte PKD2 knockout attenuates phenylephrine-induced vasoconstriction, but does not alter pressure or angiotensin II-induced vasoconstriction in hindlimb arteries. A: Mean myogenic tone at 80 mmHg illustrating that myogenic tone is similar in third-, fourth- and fifth-order mesenteric arteries and unaltered by PKD2 knockout (*Pkd2*$^{fl/fl}$: 3rd n=4; 4th n=5; 5th n=4 and *Pkd2* smKO: 3rd n=7; 4th n=4; 5th n=4). **B:** Mean data for 60 mM K^+-induced constriction in first-and second order mesenteric artery rings (*Pkd2*$^{fl/fl}$ n=5; *Pkd2* smKO n=6). **C**: Mean data for phenylephrine-induced vasoconstriction in pressurized, endothelium-denuded 4th order mesenteric arteries (*Pkd2*$^{fl/fl}$, n=3 and *Pkd2* smKO, n=3). * indicates $p<0.05$ versus *Pkd2*$^{fl/fl}$. **D**: Mean myogenic tone at 80 mmHg in endothelium-denuded 4th order mesenteric arteries (*Pkd2*$^{fl/fl}$, n=3 and *Pkd2* smKO, n=3). **E**: Mean data for angiotensin II-induced vasoconstriction in mesenteric arteries (*Pkd2*$^{fl/fl}$, n=11-12 and *Pkd2* smKO, n=10-11).

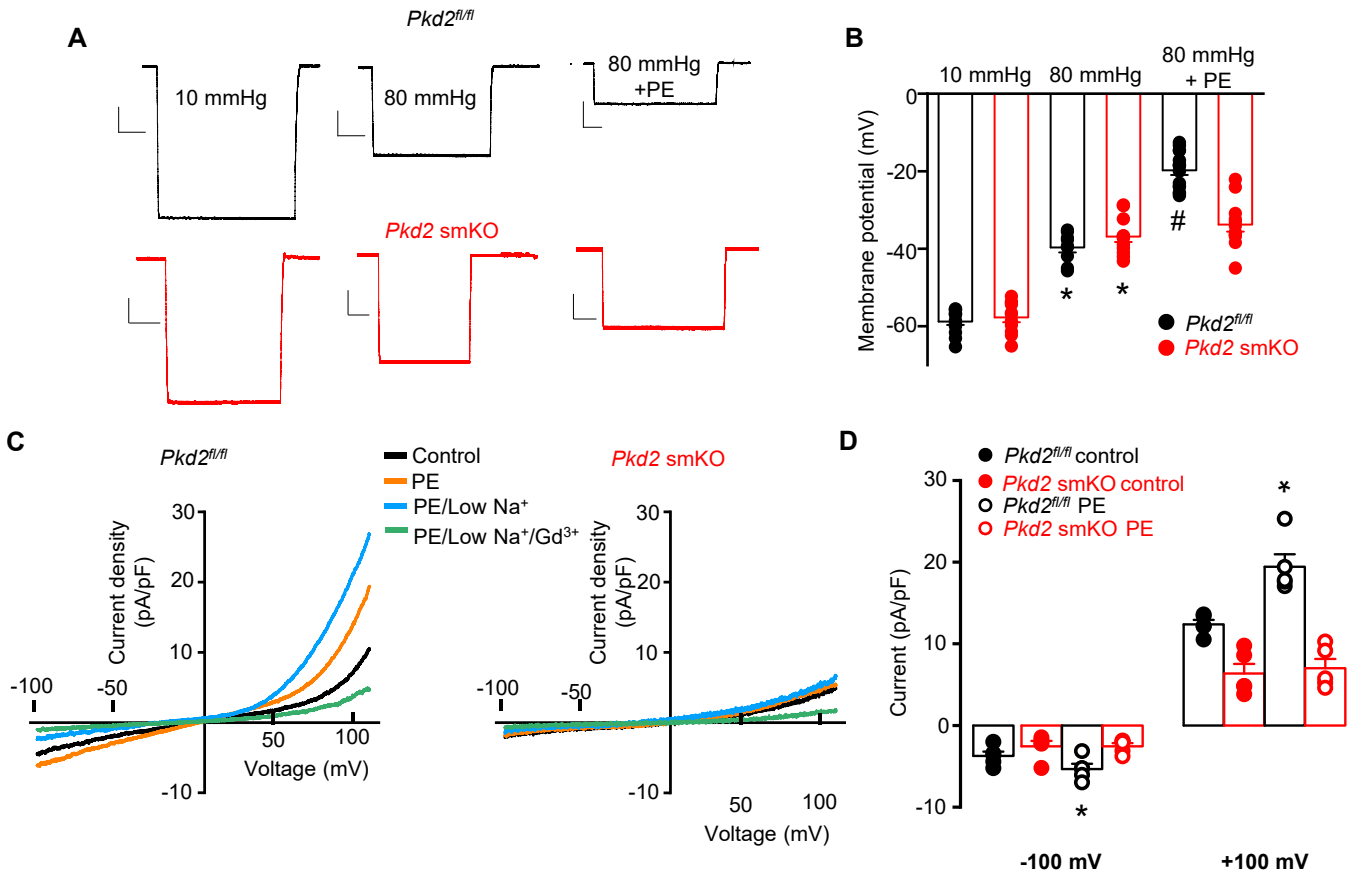

Figure 6: PKD2 channels contribute to phenylephrine-induced mesenteric artery depolarization and I_{Na} in mesenteric artery myocytes. A: Representative traces of microelectrode impalements illustrating that phenylephrine (PE, 1 µM)-induced depolarization is attenuated in mesenteric arteries of *Pkd2* smKO mice. Scale bars: Y= 10 mV, X=20 s. **B:** Mean membrane potential recordings in pressurized (10 and 80 mmHg) mesenteric arteries and in PE at 80 mmHg (*Pkd2*$^{fl/fl}$: 10 mmHg, n=13; 80 mmHg, n=9; 80 mmHg+PE, n=15. *Pkd2* smKO: 10 mmHg, n=11; 80 mmHg, n=12; 80 mmHg+PE, n=12). * P<0.05 versus 10 mmHg in the same genotype. # P<0.05 versus 80 mmHg in the same genotype. **C**: Original current recordings obtained between -100 and +100 mV in the same *Pkd2*$^{fl/fl}$ and *Pkd2* smKO myocytes in control, PE (10 µM), low Na^+ (40 mM) +PE and low Na^+ (40 mM) +PE +Gd^{3+} (100 µM). **D**: Mean paired data (*Pkd2*$^{fl/fl}$, n=5; *Pkd2* smKO, n=5; * P<0.05 versus control in the same genotype).

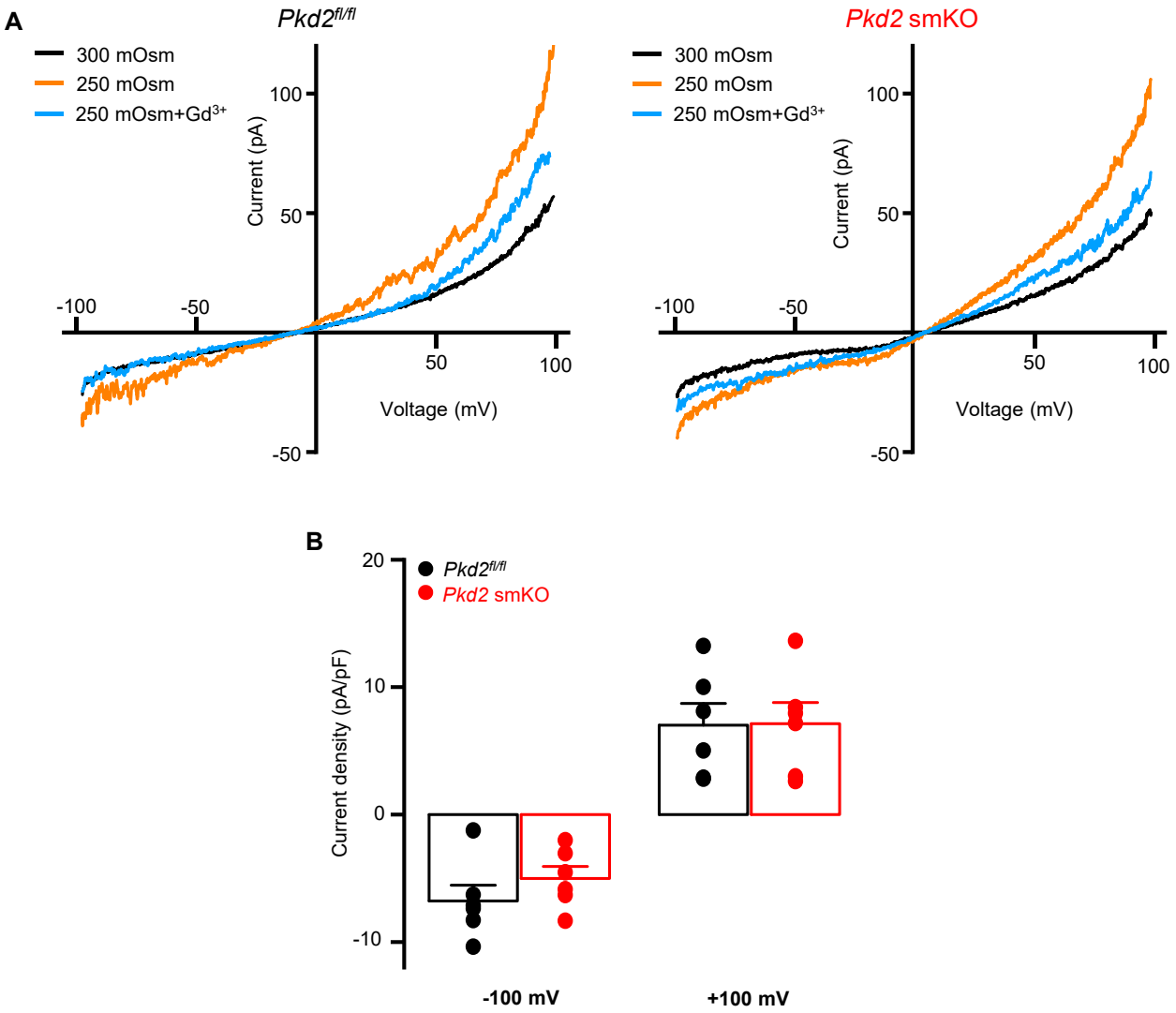

Figure 6 - figure supplement 1: PKD2 knockout does not alter swelling-activated I_{cat} in isolated mesenteric artery myocytes. A: Representative I-V relationships from the same isolated mesenteric artery myocytes of *Pkd2*$^{fl/fl}$ or *Pkd2* smKO mice in isosmosmotic (300 mOsm), hyposmotic (250 mOsm) and hyposmotic (250 mOsm) + Gd^{3+} (100 µM) solutions. **B**: Mean data for hyposmotic-activated Gd^{3+} (100 µM)-sensitive cationic current density at -100 and +100 mV (*Pkd2*$^{fl/fl}$, n=6 and *Pkd2* smKO, n=6)**.**

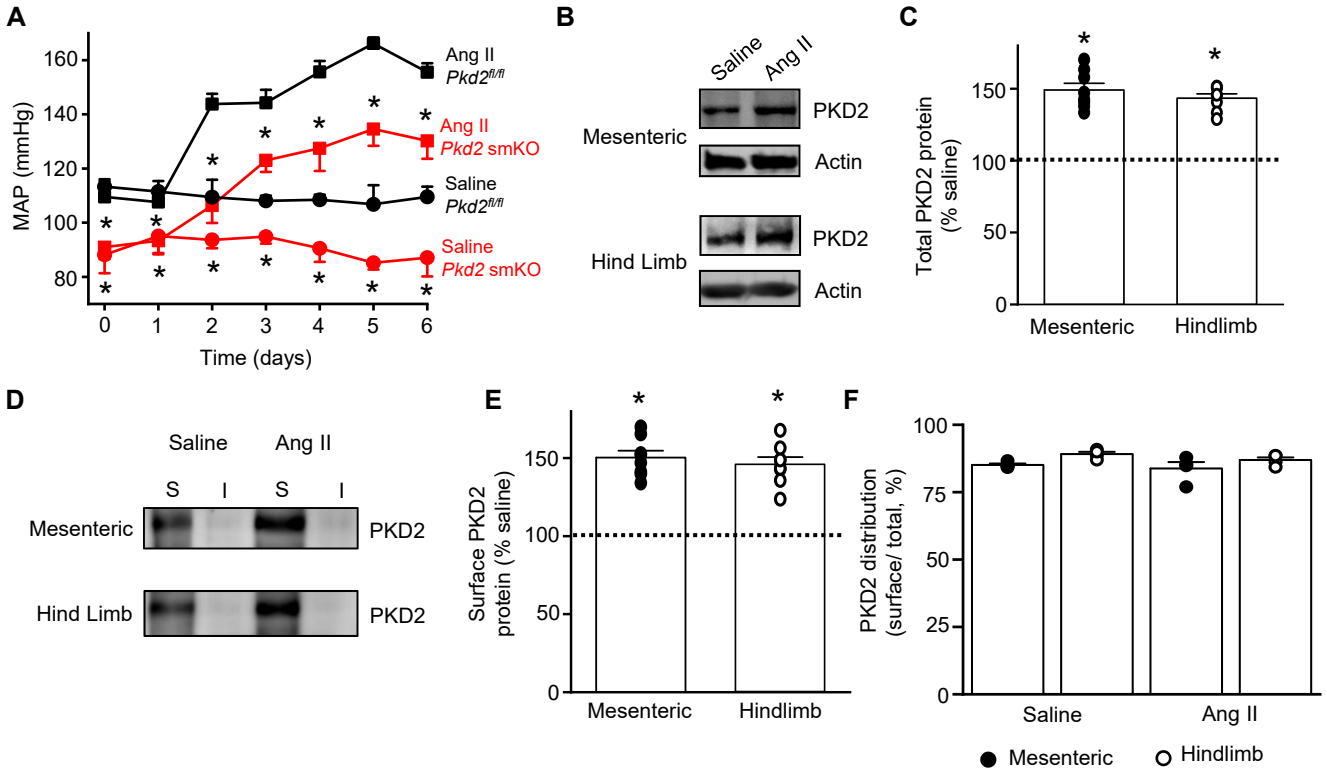

Figure 7: Angiotensin II-induced hypertension is attenuated in *Pkd2* smKO mice. A: Telemetric blood pressure time course showing the development of angiotensin II-induced hypertension in *Pkd2*$^{fl/fl}$ (n=6) and *Pkd2* smKO mice (n=9). Osmotic minipumps containing either saline or angiotensin II were implanted one day prior to day 0. * indicates p<0.05 versus *Pkd2*$^{fl/fl}$ in the same condition. **B**: Western blots illustrating total PKD2 protein in mesenteric and hindlimb arteries of saline- and angiotensin II-treated control mice. **C**: Mean total PKD2 protein in mesenteric and hindlimb arteries of angiotensin II-treated mice compared to saline control (n=8 for each group). * indicates p<0.05 versus saline in the same arterial preparation. **D**: Western blots showing surface and intracellular PKD2 protein in arteries of saline- and angiotensin II-treated mice. **E**: Mean surface PKD2 protein in mesenteric and hindlimb arteries of angiotensin II-treated mice compared to saline control (n=8 for each group). * indicates p<0.05 versus saline in the same arterial preparation. **F**: Mean data illustrating the percentage of total PKD2 located at the surface in mesenteric and hindlimb arteries of saline- and angiotensin II-treated mice (n=4 for each group).

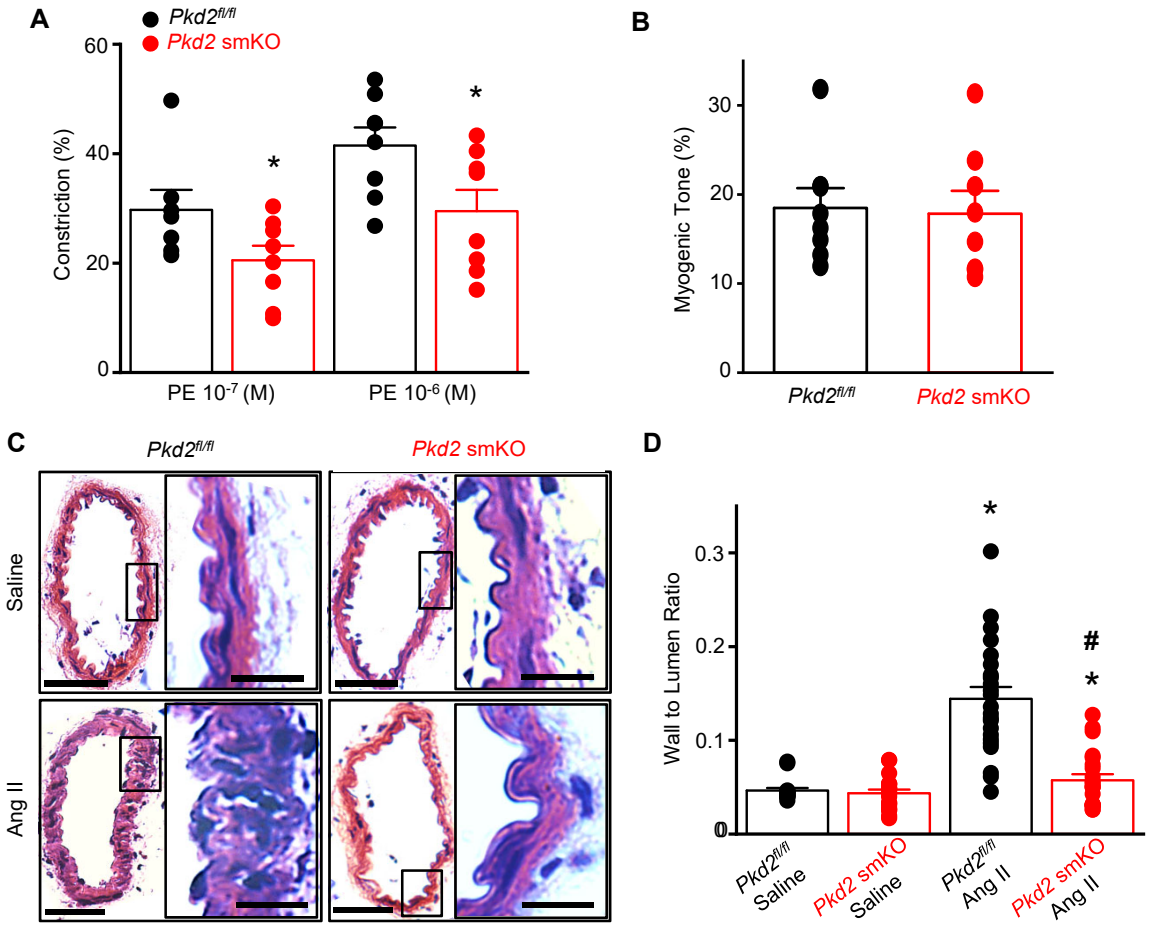

Figure 8: Arterial myocyte PKD2 knockout attenuates vasoconstriction and arterial wall remodeling during hypertension. **A**: Mean phenylephrine-induced vasoconstriction in pressurized (80 mmHg) mesenteric arteries from angiotensin II-treated mice (*Pkd2*$^{fl/fl}$, n=7-8; *Pkd2* smKO, n=8). **B**: Mean data of myogenic tone at 80 mmHg in mesenteric arteries from Ang II treated mice (*Pkd2*$^{fl/fl}$, n=8; *Pkd2* smKO, n=8). **C**: Representative H&E stained sections of fourth-order mesenteric arteries from saline and angiotensin II-treated *Pkd2*$^{fl/fl}$ and *Pkd2* smKO mice with insets. Low- and high-magnification scale bars are 50 and 25 µm, respectively. **D**: Mean data for wall-to-lumen ratio (*Pkd2*$^{fl/fl}$ saline n=17; *Pkd2* smKO saline n=20; *Pkd2*$^{fl/fl}$ ang II, n=23; *Pkd2* smKO ang II, n=22). * indicates $p<0.05$ versus saline in the same genotype and # is ang II *Pkd2* smKO versus ang II *Pkd2*$^{fl/fl}$.